



MASTER'S THESIS IN MATHEMATICS

Solving Reaction-Diffusion Equations by the Finite Element Method

December 24, 2022

Submitted by : MOHAMMAD ABDUS SAMAD

Supervised by
Prof. Dr. BERND SIMEON

TECHNICAL UNIVERSITY OF KAISERSLAUTERN, GERMANY

Abstract

This thesis deals with the solution of the reaction-diffusion equations by the finite element method.

We demonstrate the weak formulation of the reaction-diffusion equations and its existence and uniqueness. We also choose two examples of reaction-diffusion equations for numerical simulations. Later, we describe the space discretization for the finite element method in 1D and 2D cases and applications of the reaction-diffusion equations. After discretizing, we describe the non-linear reaction term and time integration.

We mainly focus on the treatment of the non-linear reaction terms in reaction-diffusion equations. We use FEniCS package to present the numerical simulation results for the reaction-diffusion equations in both 1D and 2D cases.

Acknowledgements

I am sincerely and extremely grateful to Professor Dr. Bernd Simeon for his constructive suggestions, comments and guidance. Without his guidance this research would never come to its complete shape. Also, I would like to express my grateful thanks to Dr. Falk Triebisch for taking care and providing me the necessary facilities and excellent environment in this department throughout my studies.

I am very grateful to all the faculty and staff members of the Department of Mathematics at Technical University of Kaiserslautern for their support during my study.

Finally, I would like to thank my friend Steffen Plunder, with whom I had various discussions regarding thesis work and I am also thankful to my parents, siblings and friends for their constant support and inspiration during my study period at Technical University of Kaiserslautern.

Declaration

I am Mohammad Abdus Samad, hereby state that the following master's thesis is developed and written by myself with only help of my supervisor. All information used in this work is referenced and provided as sources in the Bibliography.

Signed:

Contents

1	Introduction and Overview	1
2	Mathematical Modeling of Reaction-Diffusion Equations	3
2.1	Weak Form	4
2.2	Existence and Uniqueness	4
2.2.1	Fixed Point Methods	7
2.3	Well Posed Problems	10
3	Discretization of the Reaction-Diffusion Equations	12
3.1	Finite Element Methods in 1D	12
3.2	Finite Element Methods in 2D	14
3.2.1	Function Spaces	14
3.2.2	Variational Formulation	15
3.2.3	Galerkin Projection	15
3.2.4	Linear Triangular Elements	16
3.2.5	Compilation of Stiffness Matrix	17
3.2.6	Compilation	18
3.3	Applications of Reaction Diffusion Equations	18
3.3.1	What Can be Expected from Reaction-Diffusion Systems?	18
3.3.2	Conservative Systems	18
3.3.3	Travelling Fronts in the Belousov-Zhabotinskii Reaction	19
3.3.4	Turing Pattern Formation	21
4	Time Integration of PDEs with Nonlinear Reaction Terms	32
4.1	Treatment of Reaction Term	32
4.1.1	Finite Element Basis Functions	32
4.1.2	The Group Finite Element Method	33
4.1.3	Numerical Integration of Nonlinear Terms by Hand	33
4.2	Time Integration	34
5	Numerical Simulation	35
5.1	Designs and Components of FEniCS	35
5.2	Simulation of a Reaction-Diffusion Equation: 1D Case	36
5.3	Simulation of a Reaction-Diffusion Equation: 2D Case	38
6	Conclusion	41

Chapter 1

Introduction and Overview

Reaction-diffusion systems are the mathematical models those are related with different physical occurrence. Generally, reaction-diffusion systems are implemented in chemistry. We can find many examples in biology, physics (neutron diffusion theory), geology and ecology. In this thesis, we would describe some examples and applications of reaction-diffusion equations.

A reaction-diffusion equation comprises a reaction term and a diffusion term. Mathematically, reaction-diffusion system constitutes the form of semi-linear parabolic partial differential equations. It can be represented in the general form

$$u_t = \underbrace{D\Delta u}_{\text{diffusion}} + \underbrace{f(u)}_{\text{reaction}}$$

where $u = u(x, t)$ is the state variable and describes the density/concentration of a substance, a population... at position $x \in \Omega \subset \mathbb{R}^n$ at time t (Ω an open set). Here Δ denotes the Laplace operator. Hence, the first term on the right-hand side adds the diffusion to the system with D as a diffusion coefficient.

The second term, $f(u)$ is a smooth function $f : \mathbb{R} \rightarrow \mathbb{R}$ and describes processes which "change" the present u , i.e. something happens to it (birth, death, chemical reaction...), not just diffuse in the space.

Instead of a scalar equation, one can also introduce systems of reaction-diffusion equations, which are of the form

$$u_t = D\Delta u + f(x, u, \nabla u)$$

where $u(x, t) \in \mathbb{R}^m$. See [11], [15].

The classical three types of partial differential equations are elliptic, parabolic and hyperbolic, for which we investigate analytical solution methods for a few special situations. However, since analytical solutions cannot generally be found, or since simply no closed solution exists, now we analyze to the study of numerical solutions for partial differential equations, which at least provide an approximation to the exact solution.

Despite the wide range of numerical methods explore for approximating solutions, the finite element method is yet to be investigated. The finite element method (FEM) is a widespread used method for numerically solving differential equations in engineering and mathematical modeling. The method provides an approach to transform the complex problem (e.g.PDEs) to simpler one (e.g.ODEs, DAEs). The Finite Element Method uses the weak form of the PDE system. By means of the Galerkin projection, one searches for solutions in a finite dimensional subspace. Solutions of this finite dimensional system yield approximations of the exact solution.

Studying finite element method (FEM) is called finite element analysis (FEA). For studying engineering analysis, finite element analysis (FEA) is used in engineering as a computational tool.

The outline of the thesis as follows: In the second chapter, we focus our study to formulate the reaction-diffusion equations with boundary conditions. For implementing the finite element method (FEM), we first derive the weak formulation of the reaction-diffusion equations. After that, we focus on the existence and uniqueness of the reaction-diffusion equations and we present two examples of reaction-diffusion equations. One of them is a one dimensional reaction-diffusion equation and another is a two dimensional reaction-diffusion equation. At the end of the thesis, we try to simulate these examples through FEniCS package.

In the third chapter, we discuss one dimensional and two dimensional space discretization of reaction-diffusion equations by the finite element method (FEM). Later, we explain two applications of the reaction-diffusion equations. One is travelling fronts in the Belousov-Zhabotinskii Reaction and another is Turing pattern formation.

In the fourth chapter, after discretization, we explain the treatment of non-linear reaction term. We discuss some techniques that allow us to approximate the integrals. We also show how numerical integration of nonlinear terms can be solved by hand. At the end of this chapter, we discuss time integration.

In the fifth chapter, as a simplification of the problem, we implement our model with the FEniCS package. The FEniCS Project is a cluster of free and open source software which goal is to find automated solution of differential equations. Finally, we take two examples (1D case and 2D case) of reaction-diffusion equations and try to solve those two examples with help of the FEniCS package.

In the sixth chapter, finally we give some conclusions and an outlook of this work.

Chapter 2

Mathematical Modeling of Reaction-Diffusion Equations

The standard reaction-diffusion model deals with time evolution of chemical or biological species in a flowing medium such as water or air. The mathematical equations describing this evolution are partial differential equations (PDEs) that can be derived from mass balances. See [31]. Consider a concentration $u(x, t)$ of a certain species, with space variable $x \in \mathbb{R}$ and time $t \geq 0$. Let $h > 0$ be a small number, and consider the average concentration $\bar{u}(x, t)$ in a cell $[x - \frac{1}{2}h, x + \frac{1}{2}h]$, then

$$\bar{u}(x, t) = \frac{1}{h} \int_{x-\frac{1}{2}h}^{x+\frac{1}{2}h} u(s, t) ds = u(x, t) + \frac{1}{24} h^2 \frac{\partial^2}{\partial x^2} u(x, t) + \dots$$

We can consider the effect of diffusion. Then the change of $\bar{u}(x, t)$ is caused by gradients of the solution and the fluxes across the cell boundaries are $-d(x \pm \frac{1}{2}h, t)u_x(x \pm \frac{1}{2}h, t)$ where $d(x, t)$ the diffusion coefficient. The corresponding diffusion equation is

$$\frac{\partial}{\partial t} u(x, t) = \frac{\partial}{\partial x} \left(d(x, t) \frac{\partial}{\partial x} u(x, t) \right).$$

There may also be a local change in $u(x, t)$ due to sources, sink and chemical reactions, which is described by

$$\frac{\partial}{\partial t} u(x, t) = f(x, t, u(x, t)).$$

The overall change in concentration is described by combining these effects, leading to the diffusion-reaction equation

$$\frac{\partial}{\partial t} u(x, t) = \frac{\partial}{\partial x} \left(d(x, t) \frac{\partial}{\partial x} u(x, t) \right) + f(x, t, u(x, t)). \quad (2.1)$$

In this chapter, we consider the scalar PDE. A reaction diffusion equation comprises a reaction term and a diffusion term i.e. the typical form of (2.1) is as follows

$$u_t = \underbrace{\Delta u}_{\text{diffusion}} + \underbrace{f(u)}_{\text{reaction}} \quad \text{in } \Omega = (0, 1). \quad (2.2)$$

If we remove the reaction term from equation (2.2), then the equation represents a pure diffusion process. A complete reaction diffusion problem is usually specified by the differential equation (2.2) and some boundary conditions.

with $u = u_0$ at $t = 0$,

$$u = \tilde{u} \text{ on } \Gamma_D,$$

$$\nabla u \cdot \nu = \tau \text{ on } \Gamma_N.$$

We define the linear operator

$$Lu = u_t - \Delta u.$$

thus (2.2) becomes

$$Lu = f(u). \quad (2.3)$$

2.1 Weak Form

The first step of the finite element method is providing a weak form. It is an important utensil for analyzing mathematical models which can allow us to transfer concepts of linear algebra to solve problems in other fields such as partial differential equations. We derive it by multiplying the equation (2.2) with a test function from the space

$$V = \{v \in H^1(\Omega) : v = 0 \text{ on } \Gamma_D\}$$

and integrate over the domain Ω to get

$$\int_{\Omega} u_t v dx = \int_{\Omega} \Delta u v dx + \int_{\Omega} f(u) v dx.$$

Using the integration by parts and applying the boundary conditions, we get

$$\begin{aligned} &\Rightarrow \int_{\Omega} u_t v dx = - \int_{\Omega} u' v' dx + \int_{\partial\Omega} \langle \nabla u, \nu \rangle v d\sigma + \int_{\Omega} f(u) v dx \\ &\Rightarrow \int_{\Omega} u_t v dx + \int_{\Omega} u' v' dx = \int_{\partial\Omega} \langle \nabla u, \nu \rangle v d\sigma + \int_{\Omega} f(u) v dx. \end{aligned} \quad (2.4)$$

where ν is the outward pointing normal vector.

2.2 Existence and Uniqueness

In this section, we compare different solutions of initial boundary problems in a more general context. For existence and uniqueness of reaction-diffusion equations, we also study some general theorems. We present comparison theorem for Cauchy problems and comparison theorem for initial boundary value problems. This section is based on the reference [26].

Theorem 2.1. (Comparison theorem for Cauchy Problems) Let \underline{u} and \bar{u} be regular sub and super solutions for the Cauchy problem

$$Lu = f(u) \text{ in } Q_T \cup S_T = (0, T] \times \mathbb{R}^n$$

$$u(0, x) = u_0(x) \text{ in } S_0 = \{0\} \times \mathbb{R}^n$$

and $\underline{u} - \bar{u}$ be bounded. Let further f be uniformly Lipschitz continuous. Then

1. $\underline{u} \leq \bar{u}$ in \bar{Q}_T (Weak comparison theorem).
2. Either $\underline{u} < \bar{u}$ in $Q_T \cup S_T$ (Strong comparison theorem).
Or $\underline{u} \equiv \bar{u}$ in $Q_{t_*} \cup S_{t_*}$ for some $t_* \leq T$.

Theorem 2.2. (Comparison theorem for the initial boundary value problem) Let \underline{u} and \bar{u} be regular sub and super solutions for the initial boundary value problem

$$Lu = f(u) \text{ in } Q_T \cup S_T = (0, T] \times \Omega$$

$$u(0, x) = u_0(x) \text{ in } S_0 = \{0\} \times \Omega$$

$$Bu = b(t, x) \text{ in } (0, T) \times \partial\Omega = \Gamma.$$

Let further f be uniformly Lipschitz continuous and Q_T satisfy the interior ball property. Then

1. $\underline{u} \leq \bar{u}$ in \bar{Q}_T (Weak comparison theorem).
2. Either $\underline{u} < \bar{u}$ in $Q_T \cup S_T$ (Strong comparison theorem).
Or $\underline{u} \equiv \bar{u}$ in $Q_{t_*} \cup S_{t_*}$ for some $t_* \leq T$.
3. **Boundary point lemma:** if $\underline{u} = \bar{u}$ at some $P_* = (t_*, x_*) \in \Gamma$ and if Q_t has the interior ball property at P_* then

$$\text{either } \nabla \underline{u} \cdot \nu > \nabla \bar{u} \cdot \nu \text{ at } p_*$$

$$\text{Or } \underline{u} \equiv \bar{u} \text{ in } Q_{T_*} \cup S_{t_*}.$$

The following corollary allows us the uniqueness of the corresponding Cauchy problem. See [26]

Corollary 2.2.1. (Uniqueness) Consider the initial boundary value problem

$$\begin{aligned} Lu &= f(u) \text{ in } (0, T] \times \Omega \\ u(0, x) &= u_0(x) \text{ in } \Omega \\ Bu &= b \text{ in } (0, T) \times \partial\Omega \end{aligned} \tag{2.5}$$

with f uniformly Lipschitz continuous and $Q_T = (0, T) \times \Omega$ having the interior ball property. Then there is at most one solution of (2.5). Likewise, under the same conditions there exists at most one solution of the corresponding Cauchy problem.

Proof. Let v, w be two solutions of equation (2.5). Then they are both regular sub and super solutions. Implying the comparison theorem for the IBVPs we get

$$v \leq w \tag{2.6}$$

$$w \leq v \tag{2.7}$$

from (2.6) and (2.7) we get

$$v \equiv w.$$

□

We want to provide a method to predict the long time behavior of solutions to certain classes of reaction-diffusion equations. As an application, this method will provide global bounds for the solution of the reaction-diffusion equations. See [26].

Definition 2.3. Invariant Set : Consider the spatially invariant system

$$\begin{aligned} u_t &= f(u), \\ u : (0, T) &\rightarrow \mathbb{R}^m, \\ u(0) &= u_0. \end{aligned} \tag{2.8}$$

An invariant set of (2.8) is a set $\Sigma \subset \mathbb{R}^m$ such that if u is a solution of $u_t = f(u)$ in $0 < t < T \leq \infty$ with initial condition $u(0) \in \Sigma$, then $u(t) \in \Sigma$ for $0 \leq t \leq T$.

Similarly, an invariant set of the initial boundary value problem (2.5) is a set $\Sigma \subset \mathbb{R}$ such that if u is a solution for

$$\begin{aligned} u_t &= \Delta u + f(u) \text{ in } Q_T \cup S_T \\ \text{with } u(0, x) &\in \Sigma \quad \forall (0, x) \in S_0 \\ \text{and } Bu(t, x) &\in c(t, x)\Sigma := \{c(t, x)v : v \in \Sigma\} \end{aligned}$$

Then

$$u(t, x) \in \Sigma \text{ for each } (t, x) \in \bar{Q}_T.$$

An invariant set for the corresponding Cauchy problem can be defined analogously but asking for u to be a bounded solution. Then the following result holds : See [26]

Theorem 2.4. Consider the initial boundary value problem (2.5) with Q_t having the interior ball property or the Cauchy problem

$$\begin{aligned} u_t &= \Delta u + f(u) \text{ in } (0, T] \times \mathbb{R}^n \\ u(0, x) &= u_0(x) \text{ in } \mathbb{R}^n \end{aligned} \tag{2.9}$$

where in both cases f is Lipschitz. Furthermore, let α, β constant such that $f(\beta) \leq 0 \leq f(\alpha)$. Then $\Sigma = \{v : \alpha \leq v \leq \beta\}$ is an invariant set for (2.5) or (2.9).

Proof. Let u be a solution of (2.5).

Then u in $c(\bar{Q}_T)$ is bounded.

Therefore f is uniformly Lipschitz on the relevant domain.

Let β and α are super and sub solution of (2.9)

$$L\alpha - f(\alpha) = -f(\alpha) \leq 0 \Rightarrow \alpha \text{ sub solution}$$

$$L\beta - f(\beta) = -f(\beta) \geq 0 \Rightarrow \beta \text{ super solution}$$

Thus implies that $\alpha \leq u(t, x) \leq \beta$

i.e. $u(t, x) \in \Sigma \quad \forall (t, x) \in \bar{Q}_T$.

Thus Σ is an invariant. □

With these above assumptions, it is quite easy to show global existence of a solution. See [26].

Theorem 2.5. (Global Existence) Let f be Lipschitz and Q_T have the interior ball property (if analysing an initial boundary value problem). Further, let α, β finite constant such that $f(\beta) \leq 0 \leq f(\alpha)$, $u(0, x) \in \Sigma = \{u : \alpha \leq u \leq \beta\}$ (and $\beta u \in c\Sigma$ on Γ , if initial boundary value problem). Then there exists a solution to the initial boundary value problem (2.5) or a bounded solution to (2.9), for all times. In both cases the obtained solution is unique by corollary 2.2.1.

Proof. Whenever the solution u exists, Σ is an invariant set for all times. Thus $\alpha \leq u \leq \beta$ (since α is sub solution, β is super solution to (2.5).

Thus $f(u)$ is uniformly Lipschitz in the corresponding domain. Let us define the sequences $(v^n)_n, (w^n)_n$ such that

$$\begin{aligned} v^0 &= \alpha, \quad Lv^n + \lambda v^n = f(v^{n-1}) + \lambda v^{n-1} \\ w^0 &= \beta, \quad Lw^n + \lambda w^n = f(w^{n-1}) + \lambda w^{n-1} \end{aligned} \tag{2.10}$$

where λ denotes the Lipschitz constant of f and v^n, w^n satisfy the ICs and BCs of (2.5).

Our goal is to show the convergence of $(v^n)_n$ and $(w^n)_n$. We claim that $(v^n)_n$ is monotonically increasing and $(w^n)_n$ monotonically decreasing.

Indeed, by an induction argument. We assume

$$P(n) : v^{n+1} - v^n \geq 0$$

$$P(0) : v^1 - v^0 \geq 0$$

Induction Step : We have to show $P(n-1)$ holds for $P(n)$. We compute

$$Lv^{n+1} + \lambda v^{n+1} = f(v^n) + \lambda v^n \quad (2.11)$$

$$Lv^n + \lambda v^n = f(v^{n-1}) + \lambda v^{n-1} \quad (2.12)$$

Subtracting (2.12) from (2.11) we get

$$\begin{aligned} L(v^{n+1} - v^n) + \lambda(v^{n+1} - v^n) &= f(v^n) - f(v^{n-1}) + \lambda(v^n - v^{n-1}) \\ \Rightarrow L(v^{n+1} - v^n) + \lambda(v^{n+1} - v^n) &\geq -\lambda(v^n - v^{n-1}) + \lambda(v^n - v^{n-1}) \\ \Rightarrow L(v^{n+1} - v^n) + \lambda(v^{n+1} - v^n) &\geq 0 \end{aligned}$$

Initial conditions, boundary conditions hold for all v^n, v^{n+1}

$$\Rightarrow v^{n+1} - v^n \geq 0$$

Thus $(v^n)_n \nearrow$ is monotonically increasing.

Analogously $w^{n+1} - w^n \leq 0$

Thus $(w^n)_n \searrow$ is monotonically decreasing .

Now we have a monotonic increasing $\{v^n\}$ and a monotonic decreasing $\{w^n\}$, the limits $v = \lim_{n \rightarrow \infty} v^n$ and $w = \lim_{n \rightarrow \infty} w^n$ exists. But as there is only a unique solution of the problem i.e. it is $v = w$. \square

2.2.1 Fixed Point Methods

We study the applicability of topological fixed point theorems to non-linear partial differential equations. There are at least three distinct classes of such abstract theorems that are useful. See [9] These are the followings:

1. Fixed point theorems for strict contractions.
2. Fixed point theorems for compact mappings.
3. Fixed point theorems for order-preserving operators.

We present below applications of types (1) or (2).

Theorem 2.6. (Banach's Fixed Point Theorem) Let X denotes a Banach space. Assume

$$A : X \rightarrow X$$

is a nonlinear mapping and suppose that

$$\|A[u] - A[\tilde{u}]\| \leq \gamma \|u - \tilde{u}\| \quad (u, \tilde{u} \in X) \quad (2.13)$$

for some constant $\gamma < 1$. Then A has a unique fixed point. We say that A is a strict contraction of (2.13) holds.

Proof. Fix any point $u_0 \in X$ and thereafter iteratively define $u_{k+1} = A[u_k]$ for $k = 0, 1, \dots$. Then

$$\|A[u_{k+1}] - A[u_k]\| \leq \gamma \|u_{k+1} - u_k\| = \gamma \|A[u_k] - A[u_{k-1}]\|,$$

and so

$$\|A[u_{k+1}] - A[u_k]\| \leq \gamma^k \|A[u_0] - u_0\|$$

for $k = 1, 2, \dots$. Consequently if $k \geq l$,

$$\|u_k - u_l\| = \|A[u_{k-1}] - A[u_{l-1}]\| \leq \sum_{j=l-1}^{k-2} \|A[u_{j+1}] - A[u_j]\|$$

$$\leq \|A[u_0] - u_0\| \sum_{j=l-1}^{k-2} \gamma^j.$$

Hence $\{u_k\}_{k=1}^\infty$ is a Cauchy sequence in X , and so there exists a point $u \in X$ with $u_k \rightarrow u$ in X . Clearly then $A[u] = u$. Hence u is a fixed point for A , and hypothesis (2.13) ensures uniqueness. \square

Applications of Banach's Fixed Point Theorem to nonlinear PDE usually involve perturbation arguments of various sorts: given a well-behaved linear elliptic partial differential equation, it is often straightforward to cast a small nonlinear modification as a contraction mapping. The hallmark of such proofs is the occurrence of a parameter which must be taken small enough to ensure the strict contraction property.

Sometimes however we can break down a given problem into subproblems, each with a small parameter. See [9].

Example 1. (Reaction diffusion equations) Let us investigate the solvability of the initial/boundary-value problem for the reaction-diffusion system

$$\begin{aligned} u_t - \Delta u &= f(u) \quad \text{in } U_T, \\ u &= 0 \quad \text{on } \partial U \times [0, T], \\ u &= g \quad \text{on } U \times \{t = 0\}. \end{aligned} \tag{2.14}$$

Here $u = (u^1, \dots, u^m)$, $g = (g^1, \dots, g^m)$, and as usual $U_T = U \times (0, T]$, where $U \in \mathbb{R}^n$ is open and bounded, with smooth boundary. The time $T > 0$ is fixed. We assume that the initial function g belongs to $H_0^1(U; \mathbb{R}^m)$. Concerning the nonlinearity, let us suppose

$$f : \mathbb{R}^m \rightarrow \mathbb{R}^m \text{ is Lipschitz continuous} \tag{2.15}$$

This hypothesis in particular implies

$$|f(z)| \leq C(1 + |z|) \tag{2.16}$$

for each $z \in \mathbb{R}^m$ and some constant C .

The terminology from second-order parabolic equations, we say that a function

$$u \in L^2(0, T; H_0^1(U; \mathbb{R}^m)), \text{ with } u_t \in L^2(0, T; H^{-1}(U; \mathbb{R}^m)), \tag{2.17}$$

is a weak solution of (2.14) provided

$$\langle u_t, v \rangle + a(u, v) = \langle f(u), v \rangle \quad \text{a.e. } 0 \leq t \leq T \tag{2.18}$$

for each $v \in H_0^1(U; \mathbb{R}^m)$ and

$$u(0) = g \tag{2.19}$$

In (2.18) \langle, \rangle denotes the pairing of $H^{-1}(U; \mathbb{R}^m)$ and $H_0^1(U; \mathbb{R}^m)$, $a(,)$ is the bilinear form associated with $-\Delta$ in $H_0^1(U; \mathbb{R}^m)$, and $(,)$ denotes the inner product in $L^2(U; \mathbb{R}^m)$. The norm in $H_0^1(U; \mathbb{R}^m)$ is taken to be

$$\|u\|_{H_0^1(U; \mathbb{R}^m)} = \left(\int_U |Du|^2 dx \right)^{\frac{1}{2}}.$$

By spaces involving time (2.17) implies $u \in C([0, T]; L^2(U; \mathbb{R}^m))$, after possible redefinition of u on a set of measure zero.

For finding the existence, we explore the following theorem. See [9]

Theorem 2.7 (Existence). There exists a unique solution of (2.14).

Proof. 1. We will apply Banach's Theorem in space

$$X = C([0, T]; L^2(U; \mathbb{R}^m)),$$

with the norm

$$\|v\| := \max_{0 \leq t \leq T} \|v(t)\|_{L^2(U; \mathbb{R}^m)}.$$

Let the operator A be defined as follows. Given a function $u \in X$, set $h(t) := f(u(t))$ ($0 \leq t \leq T$). In light of the growth estimate (2.16), we see $h \in L^2(0, T; L^2(U; \mathbb{R}^m))$. Consequently the theory set from second-order parabolic equations ensure that the linear parabolic PDE

$$\begin{aligned} w_t - \Delta w &= h \quad \text{in } U_T \\ w &= 0 \quad \text{on } \partial U \times [0, T] \\ w &= g \quad \text{on } U \times \{t = 0\} \end{aligned} \tag{2.20}$$

has a unique weak solution

$$w \in L^2(0, T; H_0^1(U; \mathbb{R}^m)), \quad \text{with } w_t \in L^2(0, T; H^{-1}(U; \mathbb{R}^m)). \tag{2.21}$$

Thus $w \in X$ satisfies

$$\langle w_t, v \rangle + a(w, v) = (h, v) \quad \text{a.e. } 0 \leq t \leq T \tag{2.22}$$

for each $v \in H_0^1(U; \mathbb{R}^m)$ and $w(0) = g$.

Define $A : X \rightarrow X$ by setting $A[u] = w$.

2. We now claim that

$$\text{if } T > 0 \text{ is small enough, then } A \text{ is a strict contraction.} \tag{2.23}$$

To prove this, choose $u, \tilde{u} \in X$, and define $w = A[u]$, $\tilde{w} = A[\tilde{u}]$ as above. Consequently w verifies (2.22) for $h = f(u)$, and \tilde{w} satisfies a similar identity for $\tilde{h} := f(\tilde{u})$. After calculation we get

$$\begin{aligned} \frac{d}{dt} \|w - \tilde{w}\|_{L^2(U; \mathbb{R}^m)}^2 + 2 \|w - \tilde{w}\|_{H_0^1(U; \mathbb{R}^m)} &= 2(w - \tilde{w}, h - \tilde{h}) \\ &\leq \epsilon \|w - \tilde{w}\|_{L^2(U; \mathbb{R}^m)}^2 + \frac{1}{\epsilon} \|f(u) - f(\tilde{u})\|_{L^2(U; \mathbb{R}^m)}^2 \\ &\leq \epsilon C \|w - \tilde{w}\|_{H_0^1(U; \mathbb{R}^m)}^2 + \frac{1}{\epsilon} \|f(u) - f(\tilde{u})\|_{L^2(U; \mathbb{R}^m)}^2 \end{aligned} \tag{2.24}$$

By Poincaré's inequality. Selecting $\epsilon > 0$ sufficiently small, we deduce

$$\frac{d}{dt} \|w - \tilde{w}\|_{L^2(U; \mathbb{R}^m)}^2 \leq C \|f(u) - f(\tilde{u})\|_{L^2(U; \mathbb{R}^m)}^2 \leq C \|u - \tilde{u}\|_{L^2(U; \mathbb{R}^m)}^2,$$

since f is Lipschitz. Consequently

$$\begin{aligned} \|w(s) - \tilde{w}(s)\|_{L^2(U; \mathbb{R}^m)}^2 &\leq C \int_0^s \|u(t) - \tilde{u}(t)\|_{L^2(U; \mathbb{R}^m)}^2 dt \\ &\leq CT \|u - \tilde{u}\|^2 \end{aligned} \tag{2.25}$$

for each $0 \leq s \leq T$. Maximizing the left hand side with respect to s , we discover

$$\|w - \tilde{w}\|^2 \leq CT \|u - \tilde{u}\|^2.$$

Hence

$$\|A[u] - A[\tilde{u}]\| \leq (CT)^{\frac{1}{2}} \|u - \tilde{u}\|, \tag{2.26}$$

and thus A is a strict contraction, provided $T > 0$ is so small that $(CT)^{\frac{1}{2}} = \gamma < 1$.

3. Given any $T > 0$, we select $T_1 > 0$ so small that $(CT_1)^{\frac{1}{2}} < 1$. We can then apply Banach's Fixed Point Theorem to find a weak solution u of the problem (2.14) existing on the time interval $[0, T_1]$. Since $u(t) \in H_0^1(U; \mathbb{R}^m)$ for a.e. $0 \leq t \leq T_1$, we can upon redefining T_1 if necessary assume $u(T_1) \in H_0^1(U; \mathbb{R}^m)$.
Observe that the time $T_1 > 0$ depends only upon the Lipschitz constant for f . We can therefore repeat the argument above, to extend our solution to the time interval $[T_1, 2T_1]$. Continuing, after finitely many steps we construct a weak solution existing on the full interval $[0, T]$.
4. To demonstrate uniqueness, suppose both u and \tilde{u} are two weak solutions of (2.14). Then we have $w = u, \tilde{w} = \tilde{u}$ in inequality (2.25), whence

$$\|u(s) - \tilde{u}(s)\|_{L^2(U; \mathbb{R}^m)}^2 \leq C \int_0^s \|u(t) - \tilde{u}(t)\|_{L^2(U; \mathbb{R}^m)}^2 dt$$

for $0 \leq s \leq T$. According to Gronwall's inequality, $u \equiv \tilde{u}$.

□

Interpretation : In common applications problem (2.14) records an evolution of the densities u^1, \dots, u^m of various chemicals, which both diffuse within a medium and interact with each other. The diffusion term is Δu (or more generally $(d_1 \Delta u^1, \dots, d_m \Delta u^m)$ where the constants $d_k > 0$ characterize the diffusion of the k^{th} chemical). The reaction term $f(u)$ models the chemistry.

2.3 Well Posed Problems

The proper specification of boundary and initial data is crucial for partial differential equations. Violating this can lead to the non-existence of a solution or to the case that the solution does not depend continuously on the initial data. Hadamard (1932) defined the following. See [24]

Definition 2.8. A problem is well posed, if a solution exists, is unique and depends continuously on the initial data. Otherwise the problem is called ill posed.

Example 2. We Consider the following 1D reaction-diffusion equation which is a simple model of a single step reaction with diffusion studied by Adjerd and Flaherty. See [14], [18], [22].

$$\begin{aligned} T_t &= T_{xx} + D(1 + \alpha - T)e^{-\delta/T}, \quad t > 0, \quad 0 < x < 1 \\ T_x(0, 1) &= 0, \quad T(1, t) = 1 \\ T(x, 0) &= 1, \quad 0 \leq x \leq 1 \end{aligned} \tag{2.27}$$

with $D = Re^{\delta/\alpha\delta}$ where α is the heat release and δ is the activation energy. The variable $T(x, t)$ describes the temperature profile of a chemical reaction in the one-dimensional continuum $0 \leq x \leq 1$. For numerical simulation we use the parameter for $\alpha = 1$, $\delta = 20$ and $R = 5$.

Example 3. A solution is found for the reaction-diffusion equation, called the diffusion-Brusselator equation using the decomposition method. See [20], [3].

The problem of dealing with chemical reactions of systems involving two variable intermediates, together with a number of initial and final products whose concentrations are assumed to be controlled throughout the reaction process is an important one under quite realistic conditions and is discussed by Nicolis and Prigogine in [20]. It is necessary to consider at least a cubic nonlinearity in the rate equations [21]. This model has been referred to as the trimolecular model or Brusselator [30]. It represents a useful model for study of cooperative processes in chemical kinetics. Such a trimolecular reaction step arises in the formation of ozone by atomic oxygen via a triple collision. It arises also in enzymatic reactions, and in plasma and laser physics in multiple couplings between

certain modes.

The equation is given in the form [23]

$$\begin{aligned}\frac{\partial u}{\partial t} &= B + u^2v - (A + 1)u + \alpha\left(\frac{\partial^2 u}{\partial x^2} + \frac{\partial^2 u}{\partial y^2}\right) \\ \frac{\partial v}{\partial t} &= Au - u^2V + \alpha\left(\frac{\partial^2 v}{\partial x^2} + \frac{\partial^2 v}{\partial y^2}\right)\end{aligned}\tag{2.28}$$

The problem [20] states initial conditions $u(0, x, y) = 2 + 0.25y$, $v(0, x, y) = 1 + 0.8x$, $A = 3.4$, $B = 1$, $\alpha = 0.002$, and Neumann boundary conditions $\frac{\partial u}{\partial n} = \frac{\partial v}{\partial n} = 0$ where u and v are chemical concentrations of reaction products, A and B are constant concentrations of input reagents, and α is a constant based on a diffusion coefficient and a reactor length.

Chapter 3

Discretization of the Reaction-Diffusion Equations

Since it is not possible to solve equation (2.2) analytically, we need some discretization method. One of the most efficient method for the approximation of the solution of (2.2) is the finite element method. We therefore devote this chapter to the discretization of the model problem (2.2) with finite element methods. The approach is based on discrete representation of the weak form of (2.2).

3.1 Finite Element Methods in 1D

This section is based on the reference [13], [25], [28]. To handle the discretization of (2.2) we use the method of lines. First the equations are discretized in space by means of the finite element method. In this section, we present the details of our approximation scheme.

From equation (2.4) we get

$$\int_{\Omega} u_t v dx + \int_{\Omega} u' v' dx = \int_{\partial\Omega} \langle \nabla u, \nu \rangle v d\sigma + \int_{\Omega} f(u) v dx.$$

Applying in $\Omega = (0, 1)$ and $u(0) = \tilde{u}_0$, $u'(0) = \tau$ we get,

$$\begin{aligned} \int_0^1 u_t v dx + \int_0^1 u' v' dx &= u'(1)v(1) - u'(0)v(0) + \int_0^1 f(u) v dx \\ \Rightarrow \int_0^1 u_t v dx + \int_0^1 u' v' dx &= \int_0^1 f(u) v dx - \tau v(0) \quad \forall v \in V \text{ with } v(1) = 0. \end{aligned} \tag{3.1}$$

Now, we present approximation of this weak solution numerically.

We use here a Galerkin scheme based on piecewise linear polynomials to discretize the model equations (3.1). For $N \in \{2, 3, \dots\}$, let $\{\phi_j\}_{j=0}^{N-1}$ denote the standard piecewise linear continuous basis function (i.e., the "hats basis") for the finite dimensional subspace V_k of $H^1(0, 1)$ defined on the uniform mesh $[0, \frac{1}{N-1}, \frac{2}{N-1}, \dots, 1]$. The mesh size is $k := \frac{1}{N-1}$. For $j \in \{0, 1, \dots, N-1\}$, we have

$$\phi_j(x) = \begin{cases} \frac{x - x_{j-1}}{k}, & \text{if } x_{j-1} \leq x \leq x_j \\ \frac{x_{j+1} - x}{k}, & \text{if } x_j \leq x \leq x_{j+1} \\ 0, & \text{else.} \end{cases}$$

We formulate an approximate problem as follows: Find $u_k \in C(0, T; V_k)$ such that

$$\int_0^1 \frac{\partial u_k}{\partial t} \chi dx + \int_0^1 \frac{\partial u_k}{\partial x} \frac{\partial \chi}{\partial x} dx = \int_0^1 f(u_k) \chi dx - \tau \chi(0), \text{ for all } \chi \in V_k, t \in (0, T). \tag{3.2}$$

We let

$$u_k(t, x) = \sum_{j=0}^{N-1} \alpha_j(t) \phi_j(x), \quad t \in [0, T], x \in [0, 1], \quad (3.3)$$

where

$$\alpha(t) = (\alpha_0(t), \alpha_1(t), \dots, \alpha_{N-1}(t))^T \in \mathbb{R}^N.$$

For $t = 0$, $\alpha_j(0)$, $j \in \{0, 1, \dots, N-1\}$ are the nodal values given by the initial approximation, i.e. for $j \in \{0, 1, \dots, N-1\}$, it holds:

$$\alpha_j(0) = 1. \quad (3.4)$$

Substituting (3.3) in (3.2) yields

$$\sum_{j=0}^{N-1} \alpha'_j(t) (\phi_j(x), v) + \sum_{j=0}^{N-1} \alpha_j(t) a(\phi_j(x), v) = \int_0^1 f \left(\sum_{j=0}^{N-1} \alpha_j(t) \phi_j(x) \right) v dx - \tau v(0), t \in (0, T). \quad (3.5)$$

Taking in particular, $\chi = \phi_i(x) \in V_k$, for $i \in \{0, 1, \dots, N-1\}$ in (3.5), we obtain

$$\sum_{j=0}^{N-1} \alpha'_j(t) (\phi_j(x), \phi_i(x)) + \sum_{j=0}^{N-1} \alpha_j(t) a(\phi_j(x), \phi_i(x)) = \int_0^1 f \left(\sum_{j=0}^{N-1} \alpha_j(t) \phi_j(x) \right) \phi_i(x) dx - \tau \phi_i(0), \quad (3.6)$$

$t \in (0, T)$ for all $i \in \{0, 1, \dots, N-1\}$.

We write this expression in matrix form as

$$M\alpha'(t) + A\alpha(t) = \int_0^1 f \left(\sum_{j=0}^{N-1} \alpha_j(t) \phi_j(x) \right) \phi_i(x) dx - \tau \phi_i(0), \quad (3.7)$$

where $\alpha(t) = (\alpha_0(t), \alpha_1(t), \dots, \alpha_{N-1}(t))^T \in \mathbb{R}^N$ is the unknown vector. Here, M and A are called **Mass Matrix** and **Stiffness Matrix** respectively. The matrices $M, A \in \mathbb{R}^{N \times N}$ are defined by

$$M := \int_0^1 \phi_i(x) \phi_j(x) dx, \quad i, j \in \{0, 1, 2, \dots, N-1\},$$

$$M = \frac{k}{6} \begin{bmatrix} 2 & 1 & 0 & 0 & 0 & \dots & 0 & 0 & 0 & 0 \\ 1 & 4 & 1 & 0 & 0 & \dots & 0 & 0 & 0 & 0 \\ 0 & 1 & 4 & 0 & 0 & \dots & 0 & 0 & 0 & 0 \\ \vdots & \vdots & \vdots & \vdots & \vdots & \vdots & \vdots & \vdots & \vdots & \vdots \\ \vdots & \vdots & \vdots & \vdots & \vdots & \vdots & \vdots & \vdots & \vdots & \vdots \\ 0 & 0 & 0 & 0 & \dots & 0 & 1 & 4 & 1 & 0 \\ 0 & 0 & 0 & 0 & \dots & 0 & 0 & 1 & 4 & 1 \\ 0 & 0 & 0 & 0 & \dots & 0 & 0 & 0 & 1 & 2 \end{bmatrix},$$

$$A := \int_0^1 \nabla \phi_i(x) \nabla \phi_j(x) dx,$$

$$A = \frac{1}{k} \begin{bmatrix} 1 & -1 & 0 & 0 & 0 & \dots & 0 & 0 & 0 & 0 \\ -1 & 2 & -1 & 0 & 0 & \dots & 0 & 0 & 0 & 0 \\ 0 & -1 & 2 & -1 & 0 & \dots & 0 & 0 & 0 & 0 \\ \vdots & \vdots & \vdots & \vdots & \vdots & \vdots & \vdots & \vdots & \vdots & \vdots \\ \vdots & \vdots & \vdots & \vdots & \vdots & \vdots & \vdots & \vdots & \vdots & \vdots \\ 0 & 0 & 0 & 0 & \dots & 0 & -1 & 2 & -1 & 0 \\ 0 & 0 & 0 & 0 & \dots & 0 & 0 & -1 & 2 & -1 \\ 0 & 0 & 0 & 0 & \dots & 0 & 0 & 0 & -1 & 1 \end{bmatrix}.$$

Note that the matrix M is symmetric and positive definite as well as diagonally dominant.

3.2 Finite Element Methods in 2D

To introduce finite element method in 2D, brief definition of certain spaces and norms are imperative. We are introducing the important notions as needed in the present work, we refer the readers to look [5], [7], [10] for a comprehensive introduction to finite element methods.

3.2.1 Function Spaces

We start with the definitions of some function spaces [2].

Definition 3.1. Let the domain $\Omega \in \mathbb{R}^d$ be Lebesgue measurable with non-empty interior. The class of all measurable functions u is defined as

$$L^p(\Omega) = \{u : \Omega \rightarrow \mathbb{R} \mid \int_{\Omega} |u|^p dx < \infty\}, \quad 1 \leq p < \infty.$$

We identify two functions as the same in L^p if they only differ on a set of measure zero. These spaces are equipped with the norms

$$\|u\|_{L^p(\Omega)} := \left(\int_{\Omega} |u|^p dx \right)^{\frac{1}{p}}, \quad 1 \leq p < \infty.$$

Also important are vector subspaces of $L^p(\Omega)$, the Sobolev spaces.

Definition 3.2. For a nonnegative integer k , the **Sobolev Space** $H^k(\Omega)$ is defined as

$$H^k(\Omega) := \{u \in L^2(\Omega) \mid D^\alpha u \in L^2(\Omega) \quad \forall |\alpha| \leq k\},$$

where the weak derivative D^α for $\alpha = (\alpha_1, \dots, \alpha_d) \in \mathbb{N}_0^d$ with $|\alpha| = \sum_{j=1}^d \alpha_j$ is given by

$$D^\alpha u = \partial_{x_1}^{\alpha_1} \dots \partial_{x_d}^{\alpha_d} := \frac{\partial^{|\alpha|} u}{\partial_{x_1}^{\alpha_1} \dots \partial_{x_d}^{\alpha_d}}.$$

The Sobolev space $H^k(\Omega)$ is equipped with the norm

$$\|u\|_k := \left(\int_{\Omega} \sum_{|\alpha| \leq k} |D^\alpha u|^2 dx \right)^{\frac{1}{2}}. \quad (3.8)$$

Correspondingly, a semi-norm on this space is defined as

$$|u_k| := \left(\int_{\Omega} \sum_{|\alpha| \leq k} |D^\alpha u|^2 dx \right)^{\frac{1}{2}}. \quad (3.9)$$

Of great use will be $H_T^1(\Omega)$, a closed subspace of $H^1(\Omega)$ defined as

$$H_T^1(\Omega) = \{v \in H^1(\Omega) \mid v = 0 \text{ on } \Gamma\}.$$

It consists of square integrable functions whose trace vanishes on the boundary Γ [2]. Next, we obtain the weak formulation of the model problem (2.2).

3.2.2 Variational Formulation

In order to apply the finite element method, we have already developed a computable form of our problem, the so-called weak form. We define the space for our test functions as previously

$$V = \{v \in H^1(\Omega) : v = 0 \text{ on } \Gamma_D\}.$$

From equation (2.4) we get,

$$\int_{\Omega} u_t v dx + \int_{\Omega} u' v' dx = \int_{\partial\Omega} \langle \nabla u, \nu \rangle v d\sigma + \int_{\Omega} f(u) v dx \quad \forall v \in V.$$

Find $u \in H^1(\Omega)$ with $u = \tilde{u}$ on Γ_D and $\nabla u \cdot \nu = \tau$ on Γ_N

$$\int_{\Omega} u_t v dx + \int_{\Omega} \langle \nabla u, \nabla v \rangle dx = \int_{\Gamma_N} \tau \cdot \nu d\sigma + \int_{\Omega} f(u) v dx \quad \forall v \in V. \quad (3.10)$$

Our next step is to introduce abstract notation. We define on $H^1(\Omega) \times H^1(\Omega)$ our bilinear form

$$a(u, v) := \int_{\Omega} \langle \nabla u, \nabla v \rangle dx,$$

and the linear functional

$$(u_t, v) := \int_{\Omega} u_t v dx,$$

$$l(v) := \langle f(u), v \rangle := \int_{\Omega} f(u) v dx + \int_{\Gamma_N} \tau \cdot \nu d\sigma.$$

The weak form can now be written as: find $u \in H^1(\Omega)$, such that

$$(u_t, v) + a(u, v) = \langle l, v \rangle \quad \forall v \in V. \quad (3.11)$$

Definition 3.3. A bilinear form $a(\cdot, \cdot)$ on a normed linear space H is said to be **bounded** (or **continuous**) if there exists $C < \infty$ such that

$$|a(v, w)| \leq C \|v\|_H \|w\|_H \quad \forall v, w \in H, \quad (3.12)$$

and coercive on $V \subset H$ if there exists $\alpha > 0$ such that

$$a(v, v) \geq \alpha \|v\|_H^2 \quad \forall v \in V. \quad (3.13)$$

3.2.3 Galerkin Projection

This subsection is based on the reference [24]. The time t is simply fixed and we can consider only space. Let S_h be a finite dimensional subspace of V . The Galerkin projection results in the following task: For each time step t find the approximation $u_h(\cdot, t) \in S_h$, such that

$$\langle u_h, v \rangle + a(u_h, v) = \langle l, v \rangle \quad \forall v \in S_h. \quad (3.14)$$

Further let $\{\phi_i : 1 \leq i \leq n\}$ be a basis of S_h . An element $u_h(\cdot, t)$ that can be written as

$$u_h(\cdot, t) = \sum_{i=1}^n q_i(t) \phi_i.$$

Hence the only difference to the stationary case is that the coefficients q_i are dependent on the time. Plugging the basis functions into the bilinear form and the right hand side we obtain the stiffness matrix and the load vector

$$A := (a(\phi_i, \phi_j))_{i,j=1:n}, \quad b(t) := (\langle l(t), \phi_i \rangle)_{i=1:n}.$$

The integral yields

$$\langle u_h, v \rangle = \left\langle \sum_{i=1}^n \dot{q}_i(t) \phi_i, \phi_j \right\rangle = \sum_{i=1}^n \langle \phi_i, \phi_j \rangle \dot{q}_i(t),$$

and we construct the symmetric positive definite mass matrix

$$M := (\langle \phi_i, \phi_j \rangle)_{i,j=1:n}.$$

All together we obtain by the semi discretization in space with finite elements the system of ordinary differential equations

$$M \dot{q}(t) + Aq(t) = b(t). \quad (3.15)$$

The matrix A is called stiffness matrix and symmetric positive definite.

3.2.4 Linear Triangular Elements

This subsection is based on the reference [24]. Let $\Omega \subset \mathbb{R}^2$ a domain that can be divided into triangles. We want to solve

$$u_t = \Delta u + f(u) \text{ in } \Omega.$$

The triangulation of $\bar{\Omega}$ can be written as, Fig. ,

$$\bar{\Omega} = \bigcup_k T_k, \quad T_k : \text{triangle } k.$$

Now, the subspace reads

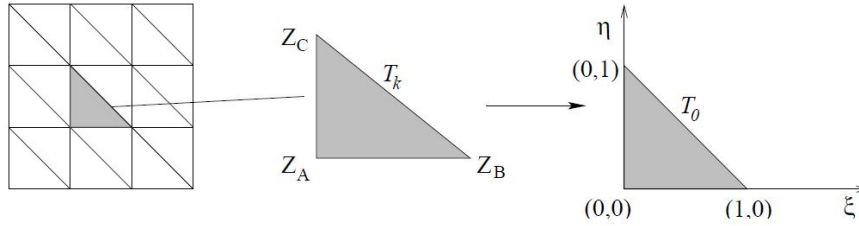


Figure 3.1: Triangulation and reference element

$$S_h := \{v \in C(\bar{\Omega}) : v|_{T_k} \text{ is linear and } v = 0 \text{ on } \partial\Omega\}. \quad (3.16)$$

A basis of S_h is given by the hat functions:

Let Z_1, Z_2, \dots, Z_n be the grid points in the interior of Ω . The hat function $\phi_i(x, y)$ is defined by

$$\phi_i(Z_j) = \delta_{ij}, \quad \phi_i|_{T_k} \text{ is linear for all } T_k.$$

Actually, ϕ_i is non-zero only in those elements that have a common corner with the point Z_i . This means that the basis functions have a small support.

The set of hat functions forms a nodal basis, i.e.

$$u_h(Z_j) = \sum_{i=1}^n \phi_i(Z_j) q_i(t) = q_j,$$

which means that the approximation in Z_j equals the coefficient q_j .

3.2.5 Compilation of Stiffness Matrix

This subsection is based on the reference [24]. Restricted to T_k with corners/vertices Z_A, Z_B, Z_C the numerical approximation reads

$$u_h|_{T_k}(x, y) = \phi_A(x, y)q_A + \phi_B(x, y)q_B + \phi_C(x, y)q_C,$$

since all other basis functions vanish in T_k . The assembly or compilation of the stiffness matrix A requires the entries

$$A_{ij} = a(\phi_i, \phi_j) = \int_{\Omega} \langle \nabla \phi_i, \nabla \phi_j \rangle dx dy = \sum_k \int_{T_k} \langle \nabla \phi_i, \nabla \phi_j \rangle dx dy.$$

Instead of running through all basis functions, the usual procedure in a FEM code is based on a loop over all elements. In other words, one computes the contributions of element T_k for the stiffness matrix. As seen above, only the 3 basis functions ϕ_A, ϕ_B, ϕ_C in T_k are different from zero and thus we need the 9 integrals

$$\int_{T_k} \langle \nabla \phi_l, \nabla \phi_m \rangle dx dy \quad \text{for } l, m \in \{A, B, C\}.$$

In order to save in computations, a transformation to a reference element T_0 by means of

$$\begin{pmatrix} x \\ y \end{pmatrix} = Z_A + (Z_B - Z_A)\xi + (Z_C - Z_A)\eta$$

proves helpful. The corresponding transformation of the integral uses

$$dx dy = J d\xi d\eta,$$

$$J = \begin{vmatrix} (Z_B - Z_A)^T \\ (Z_C - Z_A)^T \end{vmatrix}.$$

In T_0 , the hat functions ϕ_A, ϕ_B, ϕ_C are called shape functions.

$$N_1(\xi, \eta) = 1 - \xi - \eta, \quad N_2(\xi, \eta) = \xi, \quad N_3(\xi, \eta) = \eta.$$

i.e. $\phi_A|_{T_k}(x, y) = N_1(\xi(x, y), \eta(x, y))$ and so forth. Integrals over T_k are thus expressed as integrals over T_0 . For example, if $\phi_A = \phi$, $\phi_B = \psi$, $N_1 = N$, $N_2 = M$

$$\begin{aligned} \int_{T_k} \langle \nabla \phi, \nabla \psi \rangle dx dy &= \int_{T_k} (\phi_x \psi_x + \phi_y \psi_y) dx dy \\ &= \int_{T_0} ((N_\xi \xi_x + N_\eta \eta_x)(M_\xi \xi_x + M_\eta \eta_x) + (N_\xi \xi_y + N_\eta \eta_y)(M_\xi \xi_y + M_\eta \eta_y)) J d\xi d\eta. \end{aligned}$$

The partial derivatives $\xi_x, \xi_y, \eta_x, \eta_y$ depend here on the geometry of T_k . After carrying out the integrations, we obtain the element stiffness matrix, which contains all 9 integrals. It is given by

$$A_k^e := c_1 \frac{1}{2} \begin{pmatrix} 1 & -1 & 0 \\ -1 & 1 & 0 \\ 0 & 0 & 0 \end{pmatrix} + c_2 \frac{1}{2} \begin{pmatrix} 2 & -1 & -1 \\ -1 & 0 & 0 \\ -1 & 0 & 0 \end{pmatrix} + c_3 \frac{1}{2} \begin{pmatrix} 1 & 0 & -1 \\ 0 & 0 & 0 \\ -1 & 0 & 1 \end{pmatrix}$$

with the geometry constants of T_k

$$\begin{aligned} c_1 &= \frac{(Z_C - Z_A)^T (Z_C - Z_A)}{J}, \\ c_2 &= -\frac{(Z_C - Z_A)^T (Z_B - Z_A)}{J}, \end{aligned}$$

$$c_3 = \frac{(Z_B - Z_A)^T (Z_B - Z_A)}{J}.$$

The entries of the load vector $b(t)$ on the right hand side of (3.15) are computed in the same element wise fashion. It holds

$$b(t) = \langle l(t), \phi_i \rangle = \int_{\Omega} \phi_i f(u) dx dy = \sum_k \int_{T_k} \phi_i f(u) dx dy,$$

and in T_k , the element load vector is provided by

$$b_k^e = \left(\int_{T_k} \phi_A f(u) dx dy, \int_{T_k} \phi_B f(u) dx dy, \int_{T_k} \phi_C f(u) dx dy, \right)^T.$$

Note that if an exact evaluation of the integrals is impossible or too expensive, numerical quadrature comes into play. In the special case $f(u) = \text{constant}$, the linear triangular element leads to

$$b_k^e = f(u) \frac{J}{6} (1, 1, 1)^T.$$

3.2.6 Compilation

The compilation loop runs then over all elements and adds the contribution of the element to those entries that involve a basis function, say ϕ_i . More precisely, let T_k an element with vertices Z_A, Z_B, Z_C and corresponding coefficients q_A, q_B, q_C . The resulting 9 contributions of the element stiffness matrix A_k^e refer to the indices

$$\begin{aligned} &(A, A), (A, B), (A, C) \\ &(B, A), (B, B), (B, C) \\ &(C, A), (C, B), (C, C) \end{aligned}$$

of the complete stiffness matrix.

3.3 Applications of Reaction Diffusion Equations

3.3.1 What Can be Expected from Reaction-Diffusion Systems?

In general, systems of reaction-diffusion equations allow for much more complex behaviour than a scalar reaction-diffusion equation does. Especially interacting reaction terms are of interest and lead to interesting behaviour. So, e.g. oscillating phenomena can evolve-as these oscillations can spread in space via diffusion and instabilities may develop spatial phenomena like pattern formation can be observed. We will see some of the typical examples below. See [19].

Furthermore, the analysis and general statements become more difficult; not all properties which are well known from the scalar case can be directly transferred to systems.

3.3.2 Conservative Systems

We start to consider a special kind of reaction-diffusion systems, the so-called conservative systems, which means: the reaction terms are "conservative". Generally, for a conservative system, a function of the dependent variables exists, which is a constant of the motion; it can be interpreted as a kind of "energy". Mathematically formulated: System $\dot{u} = f(u)$ (m-dimensional) is conservative if a function $G(u)$ exists with

$$\dot{G}(u) = \sum_{i=1}^m \frac{\partial G}{\partial u_i} \dot{u}_i = \sum_{i=1}^m \frac{\partial G}{\partial u_i} f_i(u) = 0.$$

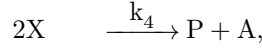
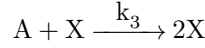
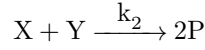
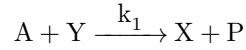
Of course, such conservative systems have special properties; e.g. they often have oscillatory solutions. Often, they are "easy" to analyse, but from a modelling point of view, there are also disadvantages, as e.g. structural instability (as known from the classical predator-prey model). See [6].

3.3.3 Travelling Fronts in the Belousov-Zhabotinskii Reaction

The Belousov-Zhabotinskii reaction is a quite famous chemical reaction system which is able to show up oscillations. Also in the spatial context, it is quite interesting to consider, as it may show up wave phenomena and pattern formation phenomena. See [19].

Goal: A model for a propagating front of a wave of chemical concentration in the Belousov-Zhabotinskii reaction:

The (simplified) chemical reaction scheme behind looks as follows:



k_i are the rate constants of the chemical reactions; the product P is not needed for the mathematical analysis. Concentration of A is assumed to be constant. Using the law of mass action and including diffusion for x and y yields as reaction diffusion system:

$$\begin{aligned} \frac{\partial x}{\partial t} &= k_1 a y - k_2 x y + k_3 a x - k_4 x^2 + D \frac{\partial^2 x}{\partial s^2} \\ \frac{\partial y}{\partial t} &= -k_1 a y - k_2 x y + D \frac{\partial^2 y}{\partial s^2} \end{aligned}$$

(remark that s denotes the space variable here). The system can be nondimensionalised,

$$u = \frac{k_4 x}{k_3 a}, v = \frac{k_2 y}{k_3 a r}, s^* = \left(\frac{k_3 a}{D}\right)^{\frac{1}{2}} s, t^* = k_3 a t, L = \frac{k_1 k_4}{k_2 k_3}, M = \frac{k_1}{k_3}, b = \frac{k_2}{k_4},$$

and then looks like (removing the asterisks for simplicity)

$$\frac{\partial u}{\partial t} = L r v + u(1 - u - r v) + \frac{\partial^2 u}{\partial s^2} \quad (3.17)$$

$$\frac{\partial v}{\partial t} = -M v - b u v + \frac{\partial^2 v}{\partial s^2}. \quad (3.18)$$

When realistic parameters are used, then L and M are of order 10^{-4} , where as b is of order 1; r is something between 5 and 50 (it has to do something with the given bromide ion concentration).

The (spatially homogeneous) stationary states can be easily computed:

$$(u, v) = (0, 0) \text{ and } (u, v) = (1, 0).$$

First approximation: Due to $L \ll 1$ and $M \ll 1$, the corresponding terms are neglected, which yields a model for the leading edge of travelling waves in the Belousov-Zhabotinskii reaction:

$$\frac{\partial u}{\partial t} = u(1 - u - r v) + \frac{\partial^2 u}{\partial s^2} \quad (3.19)$$

$$\frac{\partial v}{\partial t} = -b u v + \frac{\partial^2 v}{\partial s^2} \quad (3.20)$$

Remark 3.4. In this approximated model, all states of the form $(0, S)$ ($S > 0$ arbitrary) correspond to stationary solutions

Search for travelling wavefront solutions of (3.19), (3.20): Boundary conditions:

$$u(-\infty, t) = 0, \quad v(-\infty, t) = 1, \quad u(\infty, t) = 1, \quad v(\infty, t) = 0.$$

We look for a wave moving to the left.

Short remark in between: If we set

$$v = \frac{1-b}{r}(1-u), \quad b \neq 1, r \neq 0,$$

then the system (3.19) and (3.20) obviously reduces to the well-known

$$\frac{\partial u}{\partial t} = bu(1-u) + \frac{\partial^2 u}{\partial s^2},$$

the Fisher equation. For this case, we know already many details; e.g. the possible travelling speeds ($c \geq 2\sqrt{b}$), for non negativity we need $b < 1$; the asymptotic speed dependent on the initial condition was considered, which was (in the notation here) for an initial condition of type

$$u(s, 0) \sim O(\exp(-\beta s)) \quad \text{for } s \rightarrow \infty$$

$$c = \begin{cases} \beta + \frac{b}{\beta}, & \text{for } 0 < \beta \leq \sqrt{b} \\ 2\sqrt{b}, & \text{for } \beta > \sqrt{b} \end{cases}$$

Of course, assuming $v = \frac{1-b}{r}(1-u)$ is not very realistical; nevertheless, the Fisher equation can be useful for further analysis.

As initial conditions we introduce

$$u(s, 0) = \begin{cases} 0 & \text{for } s < s_1 \\ h(s) & \text{for } s_1 < s < s_2 \\ 1 & \text{for } s_2 < s \end{cases} \quad (3.21)$$

where $h(s)$ is a positive monotonic continuous function with $h(s_1) = 0$ and $h(s_2) = 1$ (so the desired boundary conditions can be satisfied/smooth transition possible). Then, the solution of the Fisher equation with initial condition has wave speed $c = 2\sqrt{b}$.

Let $u_f(s, t)$ be the (unique) solution of

$$\frac{\partial u_f}{\partial t} = u_f(1-u_f) + \frac{\partial^2 u_f}{\partial s^2}$$

with boundary conditions

$$u_f(-\infty, t) = 0, \quad u_f(\infty, t) = 1$$

and initial conditions (3.21); its asymptotic travelling wave front solution has speed $c = 2$. Let $u(s, t)$ be a solution of (3.19), (3.20) with the given boundary conditions and initial conditions (3.21). Using the comparison theorem we get

$$u(s, t) \leq u_f(s, t) \quad \text{for all } s, t > 0.$$

Again, we take the argument that a solution which is bounded above by another function can not travel faster than the "bound-function", thus there is the upper bound $c(r, b) \leq 2$ for the wave speed of the Belousov-Zhabotinskii solution, for all r, b . One can ask further for the dependency of the wave speed on the parameters b and r . We consider some limiting cases:

- $b = 0$: The v equation becomes $v_t = v_{ss}$, just the diffusion equation, which can not have a wave solution. As u and v must have the same wave speed, it does not work in this case at all, corresponding to $c(b \rightarrow 0, r) = 0$ for $r > 0$.

- $b \rightarrow \infty$: For v , it follows directly that $v = 0$; excluding the trivial solution $u = 0$ then leads to $c(b \rightarrow \infty, r) = 2$ for all $r \geq 0$ (from the standard Fisher equation).
- $r = 0$: Then the u equation is decoupled of v and corresponds to the standard Fisher equation, with wave speed $c = 2$ for the given initial conditions; thus the relevant solution for v also needs to have wave speed 2.
- $r \rightarrow \infty$: Either $u = 0$ or $v = 0$, so no wave solution is possible, corresponding to $c(b, r \rightarrow \infty) = 0$.

Remark 3.5. Here we have a non uniform limiting situation; the limit $r \rightarrow \infty$ with $v \neq 0$ does not correspond to the situation with $v = 0$ and then letting $r \rightarrow \infty$, as in the latter case, u is governed by the Fisher equation and r does not play a role.

Of course, we can apply now the classical travelling wave approach, let

$$u(s, t) = f(z), \quad v(s, t) = g(z) \quad \text{with} \quad z = s + ct,$$

resulting in

$$\begin{aligned} f'' - cf' + f(1 - f - rg) &= 0 \\ g'' - cg' - bfg &= 0 \end{aligned}$$

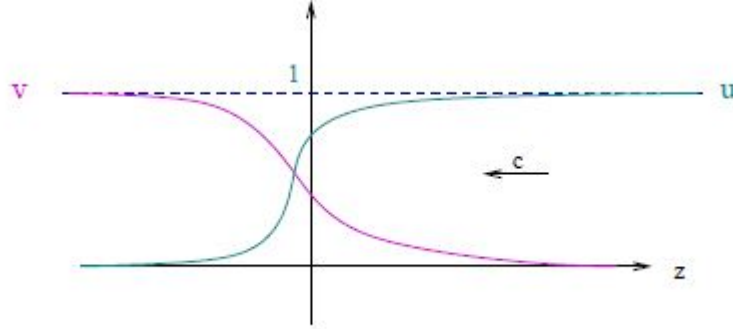
with the boundary conditions

$$f(\infty) = g(-\infty) = 1, \quad f(-\infty) = g(\infty) = 0.$$

With refined methods (using various bounds and estimation techniques for monotonic, non negative solutions), an estimation for c , dependent on the parameters r and b was found by Murray(1976):

$$\left((r^2 + \frac{2b}{3})^{\frac{1}{2}} - r\right)(2(b + 2r))^{\frac{-1}{2}} \leq c \leq 2.$$

Numerically, the typical wave fronts can be computed and look (qualitatively) as follows: The figure is taken from [15]



3.3.4 Turing Pattern Formation

Pattern formation is a ubiquitous phenomenon, not only in biology (animal coats, embryo development and morphogenesis, tumor spread, bacteria growth and dispersal), but also in chemistry (Liesegang rings, Belousov-Zhabotinsky oscillations) and physics (Rayleigh-Benard convection, liquid crystals). See [27].

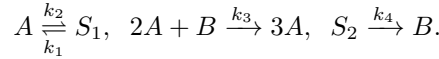
Turing proposed a mechanism for pattern formation relying on the complex interaction between reaction and diffusion of some chemicals. See [29]. Let us consider the reaction-diffusion equations describing the dynamics of two chemical concentrations A and B :

$$\partial_t A = F(A, B) + D_A \Delta A,$$

$$\partial_t B = G(A, B) + D_B \Delta B,$$

with F, G some non linear functions. Turing postulated that, if in the absence of diffusion A and B tend to a linearly stable equilibrium, then under certain conditions spatially inhomogeneous patterns can evolve by the so called diffusion driven instability. If A and B diffuse differently fast, i.e. if $D_A \neq D_B$. This seems at first reading surprising, since we know that diffusion has a stabilizing effect when met in a PDE. To see how diffusion-driven instability arises consider the two chemicals, assumed to be so-called morphogens. These are believed to be substances present in the embryonic development, which control growth pattern; recently they have been shown to exist indeed, see e.g. [1].

We can consider simple reactions between A and B , e.g. the so-called Schnakenberg model with an auto catalytic (i.e. simulating it's own production) substance A :



Using mass action kinetics we obtain for the reaction functions

$$F(A, B) = k_1 - k_2 A + k_3 A^2 B,$$

$$G(A, B) = k_4 - k_3 A^2 B.$$

We non dimensionalize by denoting

$$u = A \sqrt{\frac{k_3}{k_2}}, \quad v = B \sqrt{\frac{k_3}{k_2}}, \quad \tilde{t} = \frac{D_A t}{L^2}, \quad \tilde{x} = \frac{x}{L},$$

$$d = \frac{D_B}{D_A}, \quad a = \frac{k_1}{k_2} \sqrt{\frac{k_3}{k_2}}, \quad b = \frac{k_4}{k_2} \sqrt{\frac{k_3}{k_2}}, \quad \gamma = \frac{L^2 k_2}{D_A}.$$

Where L is a typical length scale. Then the Schnakenberg model takes the form

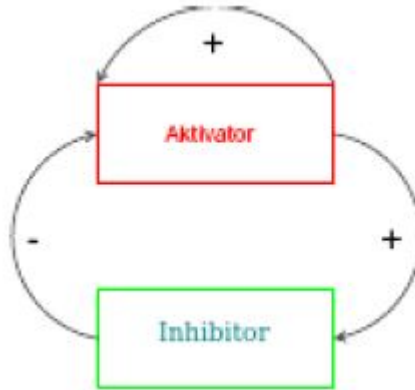
$$\partial_t u = \gamma \underbrace{(a - u + u^2 v)}_{f(u,v)} + \Delta u,$$

$$\partial_t v = \gamma \underbrace{(b - u^2 v)}_{g(u,v)} + d \Delta v.$$

Another model, still in this context is the Gierer-Meinhardt one also known as activator-inhibitor model. Thereby, a substance A (activator) interacts with another substance B (inhibitor). The activator is auto catalytic and supports the production of B . However, limiting A production, so that for the reaction functions we have

$$F(A, B) = k_1 - k_2 A + \frac{k_3 A^2}{B},$$

$$G(A, B) = k_4 A^2 - k_5 B.$$



The nondimensionalized Gierer-Meinhardt model has the form

$$\begin{aligned}\partial_t u &= \gamma \underbrace{\left(a - bu + \frac{u^2}{v}\right)}_{f(u,v)} + \Delta u \\ \partial_t v &= \gamma \underbrace{(u^2 - v)}_{g(u,v)} + d\Delta v\end{aligned}$$

with a , b and γ positive constants and with the following features:

- u is proportional to the concentration of the activator;
- v is proportional to the concentration of the inhibitor;
- $d = \frac{D_{\text{inhibitor}}}{D_{\text{activator}}}$
- $\sqrt{\gamma}$ is a measure of the domain size.
- All four quantities are positive.

Next we want to see whether a general reaction-diffusion system of the form

$$\partial_t u = \gamma f(u, v) + \Delta u, \quad (3.22)$$

$$\partial_t v = \gamma g(u, v) + d\Delta v. \quad (3.23)$$

is able to ensure diffusion-driven instability of the steady-state and to initiate a spatial pattern. We supplement (3.22) and (3.23) with boundary conditions of homogeneous Neumann type, on the boundary of a sufficient regular domain $\Omega \subset \mathbb{R}^2$, as we want to analyze patterns which are self-produced, with no input from or output to the exterior. Initial conditions are needed, as well we assume that the initial conditions are small perturbations of the steady-state of the system :

$$u(0, \mathbf{x}) = u_0 + w_1(\mathbf{x}), \quad v(0, \mathbf{x}) = v_0 + w_2(\mathbf{x}), \quad \mathbf{x} \in \Omega$$

with (u_0, v_0) being the positive solution of

$$f(u, v) = 0, \quad g(u, v) = 0.$$

Idea of Turing instability

- Without diffusion the homogeneous steady state is stable w.r.t. small perturbations.
- When including diffusion this steady state becomes unstable.

We start performing the stability analysis of our RDE system, first in the case without diffusion. We can write the perturbations of the equilibrium in vector form: $\mathbf{w} = \begin{pmatrix} u - u_0 \\ v - v_0 \end{pmatrix}$. Then we have for \mathbf{w}

$$\frac{\partial \mathbf{w}}{\partial t} = \begin{pmatrix} \frac{\partial u}{\partial t} \\ \frac{\partial v}{\partial t} \end{pmatrix} = \begin{pmatrix} \gamma f(u, v) \\ \gamma g(u, v) \end{pmatrix}.$$

Expanding the right hand side around the steady state (u_0, v_0) :

$$\begin{aligned}\frac{\partial \mathbf{w}}{\partial t} &= \gamma \begin{pmatrix} f(u_0, v_0) + f_u(u_0, v_0)(u - u_0) + f_v(u_0, v_0)(v - v_0) \\ g(u_0, v_0) + g_u(u_0, v_0)(u - u_0) + g_v(u_0, v_0)(v - v_0) \end{pmatrix} \\ &= \gamma \begin{pmatrix} f_u(u_0, v_0) + f_v(u_0, v_0) \\ g_u(u_0, v_0) + g_v(u_0, v_0) \end{pmatrix} \mathbf{w} \\ &=: \gamma \mathbf{A} \mathbf{w}.\end{aligned} \quad (3.24)$$

Remark 3.6. The previous derivatives are only valid at equilibrium, so the derived equations cannot be generalized to hold for every point (u, v) .

We look for solutions of (3.24) of the form $\mathbf{w} = e^{\lambda t}$, with λ being eigen values of the matrix $\gamma\mathbf{A}$. The steady state $\mathbf{w} = 0$ is supposed to be stable, and it is $Re\lambda < 0$ (in which case $\mathbf{w} \rightarrow 0$ for $t \rightarrow \infty$). The eigen values of $\gamma\mathbf{A}$ are obtained by solving the characteristic polynomial

$$\lambda^2 - \gamma(f_u + g_v)(u_0, v_0)\lambda + \gamma^2(f_u g_v - f_v g_u)(u_0, v_0) = 0,$$

thus

$$\lambda_1, \lambda_2 = \frac{1}{2}\gamma[(f_u + g_v)(u_0, v_0) \pm \sqrt{((f_u + g_v)(u_0, v_0))^2 - 4(f_u g_v - f_v g_u)(u_0, v_0)}].$$

Therefore, linear stability of $\mathbf{w} = 0$ occurs for

$$\text{trace}\mathbf{A} = (f_u + g_v)(u_0, v_0) < 0, \quad \det\mathbf{A} = (f_u g_v - f_v g_u)(u_0, v_0) > 0. \quad (3.25)$$

In the **presence of diffusion** the steady state $\mathbf{w} = 0$ should be unstable. If we consider the full system (3.22) and (3.23) and linearize again about (u_0, v_0) we get as above

$$\begin{aligned} \frac{\partial \mathbf{w}}{\partial t} &= \begin{pmatrix} \frac{\partial u}{\partial t} \\ \frac{\partial v}{\partial t} \end{pmatrix} = \begin{pmatrix} \gamma(f_u(u_0, v_0)(u - u_0) + f_v(u_0, v_0)(v - v_0)) + \Delta u \\ \gamma(g_u(u_0, v_0)(u - u_0) + g_v(u_0, v_0)(v - v_0)) + d\Delta u \end{pmatrix} \\ &= \begin{pmatrix} \gamma(f_u(u_0, v_0)(u - u_0) + f_v(u_0, v_0)(v - v_0)) + \Delta(u - u_0) \\ \gamma(g_u(u_0, v_0)(u - u_0) + g_v(u_0, v_0)(v - v_0)) + d\Delta(u - u_0) \end{pmatrix} \\ &= \gamma\mathbf{A}\mathbf{w} + \mathbf{D}\Delta\mathbf{w}, \end{aligned} \quad (3.26)$$

with the diffusion matrix $\mathbf{D} = \begin{pmatrix} 1 & 0 \\ 0 & d \end{pmatrix}$. This is a linear system of PDEs. To solve it we apply the method of separation of variables: $\mathbf{w}(t, \mathbf{x}) = \mathbf{X}(\mathbf{x})T(t)$. This leads to

$$\mathbf{X}(\mathbf{x})T'(t) = \gamma\mathbf{A}\mathbf{X}(\mathbf{x})T(t) + \mathbf{D}T(t)\Delta\mathbf{X}(\mathbf{x}),$$

with corresponding initial conditions and homogeneous Neumann boundary conditions. The idea is to consider a boundary eigen value problem, allowing us to substitute $\Delta\mathbf{X}(\mathbf{x})$ by a multiple of $\mathbf{X}(\mathbf{x})$ and which guarantees the boundary conditions being satisfied:

$$\begin{aligned} \Delta\mathbf{X}(\mathbf{x}) + k^2\mathbf{X}(\mathbf{x}) &= 0 \quad \text{in } \Omega \\ \nabla\mathbf{X}(\mathbf{x}) \cdot \nu &= 0 \quad \text{on } \partial\Omega. \end{aligned} \quad (3.27)$$

The eigen functions $X_k(\mathbf{x})$ depend on the considered domain (and on k); e.g. for the 1D case $\Omega = [0, a]$ we have the eigen functions $X_k(x) = c_k \cos(kx)$ with $k = \frac{n\pi}{a}$, $n \in \mathbb{N}$. With the ansatz

$$\mathbf{w}(t, x) = \sum_{k=1}^{\infty} \mathbf{X}_k(\mathbf{x})T_k(t).$$

We obtain from (3.26)

$$\sum_{k=1}^{\infty} (T'_k(t)I - \gamma T_k(t)\mathbf{A} + k^2 T_k(t)\mathbf{D})\mathbf{X}_k(\mathbf{x}) = 0.$$

Now set $T_k(t) := e^{\lambda t}$ (The time dependent solution in the case without diffusion; recall λ is an eigen value of $\gamma\mathbf{A}$) and get

$$\sum_{k=1}^{\infty} (\lambda I - \gamma\mathbf{A} + K^2\mathbf{D})e^{\lambda t}\mathbf{X}_k(\mathbf{x}) = 0.$$

For that it is sufficient to have

$$\lambda \mathbf{X}_k(\mathbf{x}) = (\gamma \mathbf{A} - k^2 \mathbf{D}) \mathbf{X}_k(\mathbf{x}), \quad \forall k \in \mathbb{N}$$

hence

$$\lambda_1(k), \lambda_2(k) = \frac{1}{2} [\text{trace}(\gamma \mathbf{A} - k^2 \mathbf{D}) \pm \sqrt{(\text{trace}(\gamma \mathbf{A} - k^2 \mathbf{D}))^2 - 4 \det(\gamma \mathbf{A} - k^2 \mathbf{D})}].$$

We keep looking for the condition of instability of the steady-state in the presence of diffusion. There obviously exists $k \in \mathbb{N}$ with $\text{Re}(\lambda(k)) > 0$. For the instability we need either

$$\text{trace}(\gamma \mathbf{A} - k^2 \mathbf{D}) > 0,$$

which is excluded due to $\text{trace}(\mathbf{A}) < 0$ in (3.25) or:

$$\det(\gamma \mathbf{A} - k^2 \mathbf{D}) < 0,$$

thus

$$h(k^2) := d(k^2)^2 - \gamma(df_u(u_0, v_0) + g_v(u_0, v_0))k^2 + \gamma^2 \det(\mathbf{A}) < 0.$$

Necessarily

$$df_u(u_0, v_0) + g_v(u_0, v_0) > 0 \quad (3.28)$$

has to hold and it suffices to have

$$\frac{(df_u(u_0, v_0) + g_v(u_0, v_0))^2}{4d} > \det(\mathbf{A}). \quad (3.29)$$

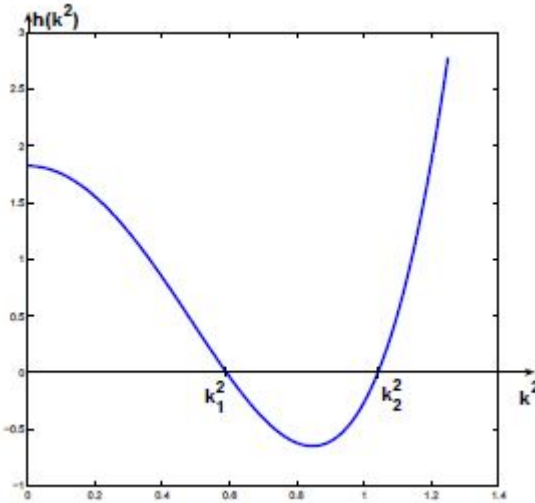
Now what is the parameter range for k^2 in order for a pattern to exist? From $h(k^2) < 0$ it follows that the range of k^2 is located in between the roots k_1^2 and k_2^2 :

$$k_1^2, k_2^2 = \frac{\gamma}{2d} [(df_u(u_0, v_0) + g_v(u_0, v_0)) \pm \sqrt{(df_u(u_0, v_0) + g_v(u_0, v_0))^2 - 4d \det(\mathbf{A})}].$$

Thus, the following inequalities have to be satisfied:

$$\gamma c_1(d, \mathbf{A}) = k_1^2 < K^2 < k_2^2 = \gamma c_2(d, \mathbf{A}) \quad (3.30)$$

with corresponding bounds c_1 and c_2 . The following figure is taken from [27]



Proposition 1. (Conditions for Turing pattern formation)

The following four conditions in (3.25), (3.28), (3.29) have to be satisfied in order to have diffusion driven instability leading to Turing pattern formation:

1. $f_u(u_0, v_0) + g_v(u_0, v_0) < 0$.
2. $f_u(u_0, v_0)g_v(u_0, v_0) - f_v(u_0, v_0)g_u(u_0, v_0) > 0$.
3. $df_u(u_0, v_0) + g_v(u_0, v_0) > 0$.
4. $[df_u(u_0, v_0) + g_v(u_0, v_0)]^2 - 4d[f_u(u_0, v_0)g_v(u_0, v_0) - f_v(u_0, v_0)g_u(u_0, v_0)] > 0$.

Remark 3.7. • f_u and g_v need to have different signs in (u_0, v_0) . Test this with the Schnakenberg and the Gierer-Meinhardt models.

- It has to hold $d > 1$, meaning

$$d = \frac{D_{\text{inhibitor}}}{D_{\text{activator}}} > 1$$

(How can we interpret this?)

In the following we assume the previous conditions to hold, so there are certain values for k^2 such that the corresponding eigen functions form the pattern. Which values of k are these and what patterns are formed, i.e. upon which parameters do these patterns depend?

To answer these questions let us think back at where the k values came from. Remember we wanted to solve (3.27). For that we have to specify the domain Ω there in. We analyze the situation of 2D rectangular domain $\Omega = [0, p] \times [0, q]$.

We get the solution

$$\mathbf{X}_{n,m}(x, y) = \mathbf{c}_{n,m} \cos\left(\frac{n\pi x}{p}\right) \cos\left(\frac{m\pi y}{q}\right),$$

satisfying the boundary conditions. Inserting this into the PDE leads to

$$k^2 = \pi^2 \left(\frac{n^2}{p^2} + \frac{m^2}{q^2} \right).$$

The inequality (3.30) for the boundaries of the k^2 range yields

$$\gamma c_1(d, \mathbf{A}) = k_1^2 < k^2 = \pi^2 \left(\frac{n^2}{p^2} + \frac{m^2}{q^2} \right) < k_2^2 = \gamma c_2(d, \mathbf{A}). \quad (3.31)$$

The solution of the PDE is then $\mathbf{w}(t, \mathbf{x}) = \sum_{k=1}^{\infty} \mathbf{X}_k(\mathbf{x}) T_k(t)$, hence in our case

$$\mathbf{w}(t, \mathbf{x}) = \sum_{n,m=1}^{\infty} \mathbf{c}_{n,m} \cos\left(\frac{n\pi x}{p}\right) \cos\left(\frac{m\pi y}{q}\right) e^{\lambda(\pi \sqrt{\frac{n^2}{p^2} + \frac{m^2}{q^2}})t}.$$

For large times we can neglect the summands not fulfilling the inequality (3.31) due to the exponential decay of the eigen functions $X_{n,m}(x, y)$. Assume there can be selected an appropriate γ such that there remains only one summand, i.e. only one pair (n, m) satisfies the inequality.

Example 4. For $(n, m) = (1, 0)$ we get a certain time

$$\mathbf{w}(t, \mathbf{x}) = \mathbf{c}_{1,0} \cos\left(\frac{\pi x}{p}\right).$$

This characterizes the picture of the perturbation $\mathbf{w}(x, y)$ on the rectangular domain $\Omega = [0, p] \times [0, q]$.

How do we get a pattern? It has been proposed by Turing that the interaction of a pair of morphogens working together as an activator and an inhibitor substance, respectively, in the

destabilizing presence of diffusion of both substances (with the inhibitor diffusing faster than the activator) can lead to animal patterns. One could think about skin cells reading out the space-time-dependent concentration of the activator and comparing it with a reference concentration. When the latter is exceeded this causes the cell to produce pigment (e.g. melanin).

Let us assume that the reference concentration is the value u_0 of the homogeneous steady-state for the activator u . In order to simplify things let us take

$$\mathbf{c}_{1,0} := (\epsilon, \epsilon) e^{\lambda(\frac{\pi x}{p})t},$$

so that we have then

$$u(t, \mathbf{x}) \simeq u_0 + \epsilon e^{\lambda(\frac{\pi x}{p})t} \cos\left(\frac{\pi x}{p}\right).$$

For values of u above u_0 a cell will produce pigment, otherwise not:

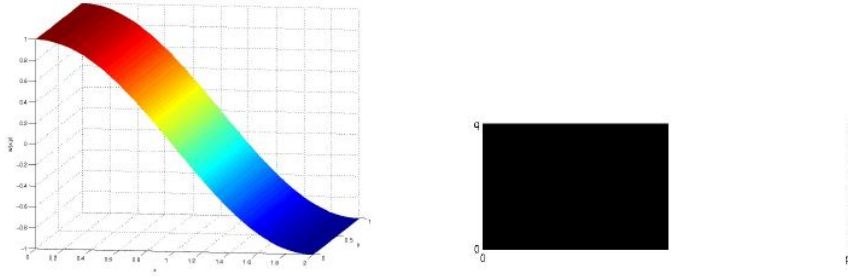


Figure 3.2: Behavior of activator u for $(n, m) = (1, 0)$ with $p = 2, q = 1$ and corresponding pattern. This figure is taken from [27].

Example 5. Considering the pair $(n, m) = (2, 0)$ we have a pattern with two black stripes due to the underlying function

$$\mathbf{w}(t, \mathbf{x}) = \mathbf{c}_{2,0}(t) \cos\left(\frac{2\pi x}{p}\right),$$

thus due to

$$u(t, \mathbf{x}) \simeq u_0 + \epsilon e^{\lambda(\frac{2\pi x}{p})t} \cos\left(\frac{2\pi x}{p}\right).$$

The x dimension is now twice as large as in example 4, thus the cosine has a supplementary possibility of changing sign.

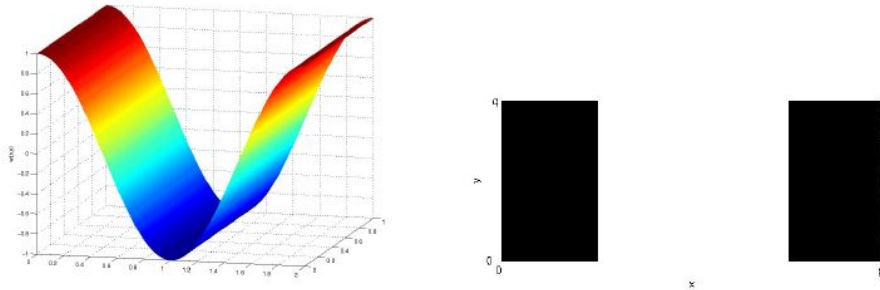


Figure 3.3: Behavior of activator u for $(n, m) = (2, 0)$ with $p = 2, q = 1$ and corresponding pattern. This figure is taken from [27].

Example 6. For $m > 0$, e.g. in the case $(n, m) = (2, 1)$, the pigment wave spreads also in the y direction, as we have a product of two cosines. The emerging checkerboard pattern allows to account for spots:

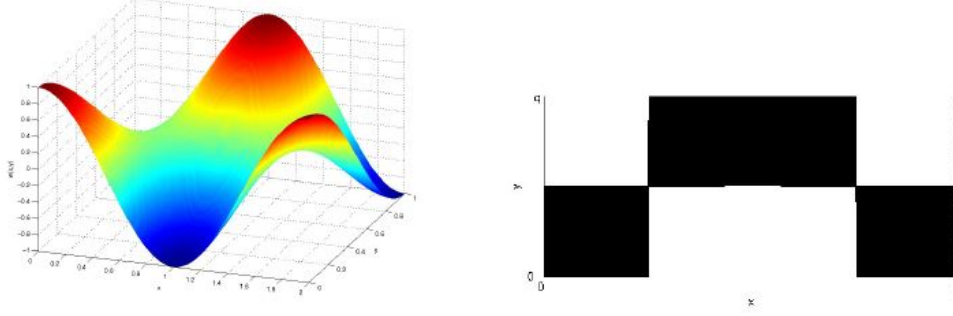


Figure 3.4: Behavior of activator u for $(n, m) = (2, 1)$ with $p = 2, q = 1$ and corresponding pattern. This figure is taken from [27].

Remark 3.8. Let us review the assumptions we made:

- We assume only one summand (i.e. only one pair (n, m)) to satisfy the inequality (3.31). To change the values for these pairs we had to change the bounds $c_1(d, \mathbf{A})$ and $c_2(d, \mathbf{A})$. As these bounds are however, fixed (due to model), we were only able to change γ .
- For large values of γ (remember this parameter was a measure of the domain size) the range in which inequality (3.31) holds increases, the lower and upper bounds allow for larger m and n .
- Larger values of m and n cause a finer checkerboard pattern, so larger animals ought to have a finer pattern.
- We took (rather artificially) the equilibrium as a threshold for the pigment production. This threshold could be however, higher or lower. What would then be the consequences for the spots/strips with pigment?
- Some felines and cows have many spots.
- Looking at the tails of some animals (e.g. of cheetahs or of genets, figure 3.7) we see the spots become stripes. This is due to the shrinking domain size γ .
- Still due to the domain size and the time dependent evolution of both domain and pattern, there are differences between patterns with spots (see figure 3.8).
- and patterns with stripes, even with intra species variety (see figure 3.9).

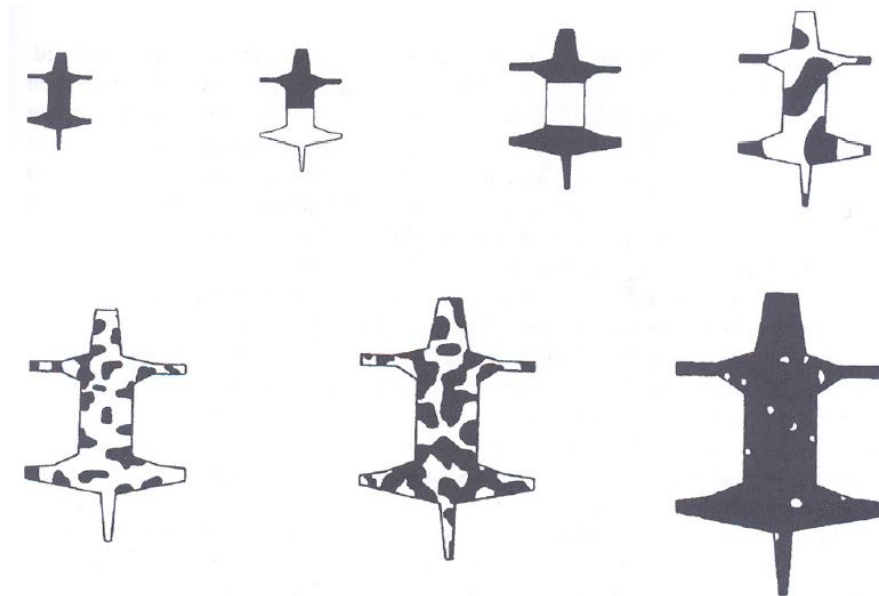


Figure 3.5: Effect of the domain size on the pattern $\gamma_1 = 1, \gamma_2 = 28, \gamma_3 = 65, \gamma_4 = 150, \gamma_5 = 500, \gamma_6 = 800, \gamma_7 = 10000$. This figure is taken from [27].



Figure 3.6: Which animal has a larger γ , what about m, n ? This figure is taken from [27].

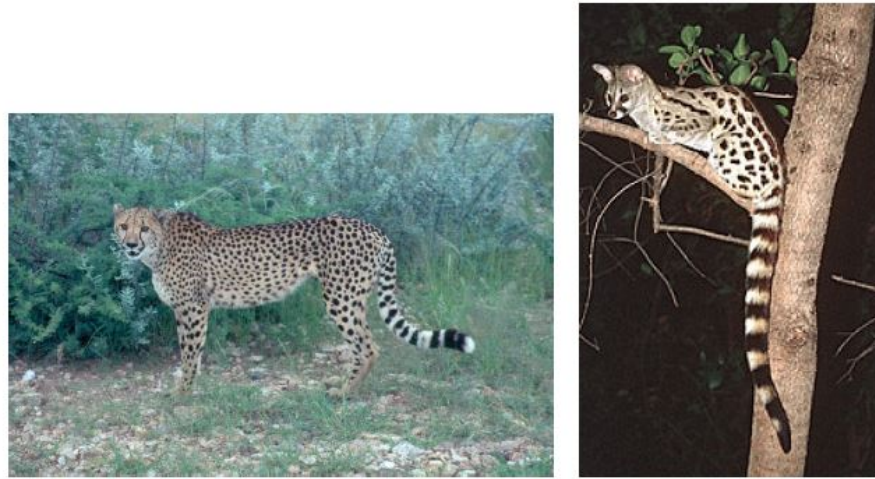


Figure 3.7: On the tail of a Cheetah the spots become stripes towards the tip of the tail. The tail of a genet is completely striped. This figure is taken from [27].

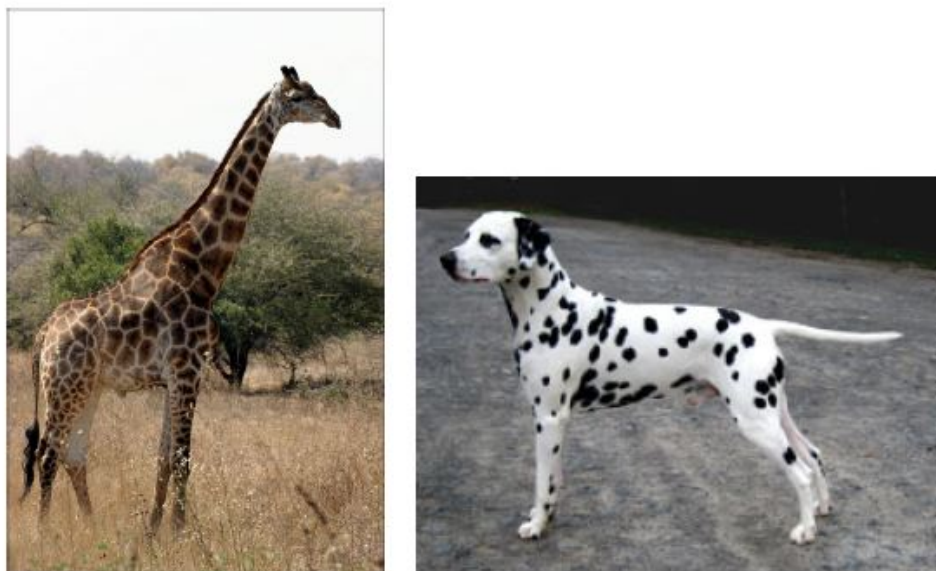


Figure 3.8: Spots on a Giraffe are very large compared to spots on a Dalmatian. This figure is taken from [27].

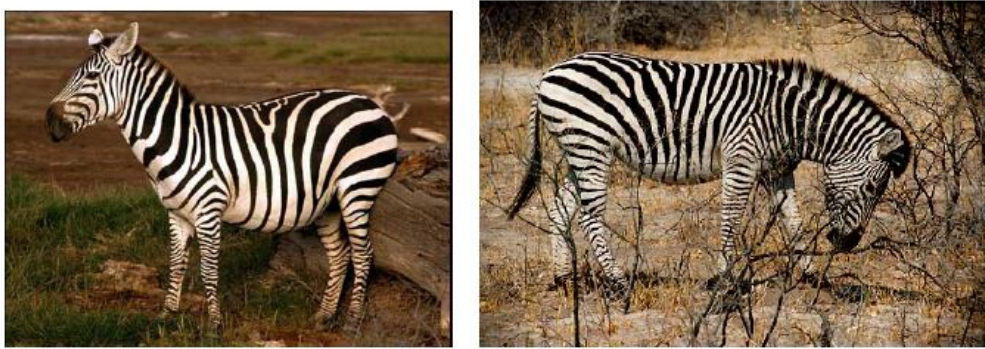


Figure 3.9: Stripes on different zebra races: the left race develops its pattern earlier in the embryonal stage, which leads to less, but broader stripes. This figure is taken from [27].

Chapter 4

Time Integration of PDEs with Nonlinear Reaction Terms

4.1 Treatment of Reaction Term

The integrals in nonlinear finite element equations are computed by numerical integration rules in computer programs, so the formulas for the variational form are directly transferred to numbers. It is also of interest to understand the nature of the system of difference equations that arises from the finite element method in nonlinear problems and to compare with corresponding expressions arising from finite difference discretization. To see the structure of the difference equations implied by the finite element method, we have to find symbolic expressions for the integrals, and this is extremely difficult since the integrals involve the unknown function in nonlinear problems. However, there are some techniques that allow us to approximate the integrals and work out symbolic formulas that can be compared with their finite difference counterparts. This section is based on the reference [16].

4.1.1 Finite Element Basis Functions

Introduction of finite element basis functions φ_i means setting

$$\psi_i = \varphi_{\nu(i)}, \quad i \in \mathcal{I}_s,$$

where degree of freedom number $\nu(i)$ in the mesh corresponds to unknown number $i(c_i)$. Using all the basis functions except the last at $i = N_n$, i.e., $\mathcal{I}_s = \{0, \dots, N_n - 1\}$, and $\nu(j) = j$. The expansion of u can be taken as

$$u = D + \sum_{j \in \mathcal{I}_s} c_j \varphi_{\nu(j)},$$

but it is more common in a finite element context to use a boundary function $B = \sum_{j \in I_b} U_j \varphi_j$, where U_j is prescribed Dirichlet condition for degree of freedom number j and U_j is the corresponding value

$$u = D \varphi_{N_n} + \sum_{j \in \mathcal{I}_s} c_j \varphi_{\nu(j)}.$$

In the general case with u prescribed as U_j at some nodes $j \in I_b$, we get

$$u = \sum_{j \in I_b} U_j \varphi_j + \sum_{j \in \mathcal{I}_s} c_j \varphi_{\nu(j)},$$

where $c_j = u(x_{\nu(j)})$. That is $\nu(j)$ maps unknown number j to the corresponding node number $\nu(j)$ such that $c_j = u(x_{\nu(j)})$.

4.1.2 The Group Finite Element Method

Finite element approximation of functions of u . Since we already expand u as $\sum_j \varphi_j u(x_j)$, we may use the same approximation for other functions as well. For example,

$$f(u) \approx \sum_j f(x_j) \varphi_j,$$

where $f(x_j)$ is the value of f at node j . Since f is a function of u , $f(x_j) = f(u(x_j))$. Introducing u_j as a short form for $u(x_j)$, we can write

$$f(u) \approx \sum_j f(u_j) \varphi_j.$$

This approximation is known as the group finite element method or the product approximation technique. The index j runs over all node numbers in the mesh. The principle advantages of the group finite element method are two fold.

1. Complicated nonlinear expressions can be simplified to increase the efficiency of the numerical computations.
2. One can derive forms of the difference equations arising from the finite element method in nonlinear problems. The symbolic form is useful for comparing finite element and finite difference equations of nonlinear differential equation problems.

Exploring point 2, the finite element method creates more complex expressions in the resulting linear system (the difference equations) than the finite difference method does. It turns out that it is very difficult to see what kind of terms in the difference equations that arise from $\int f(u) \varphi_i dx$ without using the group finite element method or numerical integration utilizing the nodes only.

However, that an expression like $\int f(u) \varphi_i dx$ causes no problems in a computer program as the integral is calculated by numerical integration using an approximation of u in $f(u)$ such that the integrand can be sampled at any spatial point.

4.1.3 Numerical Integration of Nonlinear Terms by Hand

Let us reconsider the term $\int f(u) v dx$ as treated in the space discretization section, but now we want to integrate this term numerically. Such an approach can lead to easy-to-interpret formulas if we apply a numerical integration rule that samples the integrand at the node points x_i only, because at such points, $\varphi_j(x_i) = 0$ if $j \neq i$, which leads to great simplifications.

The term takes the form

$$\int_0^L f \left(\sum_k u_k \varphi_k \right) \varphi_i dx.$$

Evaluation of the integrand at a node x_l leads to a collapse of the $\sum_k u_k \varphi_k$ to one term because

$$\sum_k u_k \varphi_k(x_l) = u_l.$$

$$f \left(\sum_k u_k \underbrace{\varphi_k(x_l)}_{\delta_{kl}} \right) \underbrace{\varphi_i(x_l)}_{\delta_{il}} = f(u_l) \delta_{il},$$

where we have used the Kronecker delta $\delta_{ij} = 0$ if $i \neq j$ and $\delta_{ij} = 1$ if $i = j$.

Considering the Trapezoidal rule for integration, where the integration points are the nodes, we have

$$\int_0^L f \left(\sum_k u_k \varphi_k(x) \right) \varphi_i(x) dx \approx h \sum_{l=0}^{N_n-1} f(u_l) \delta_{il} - \mathcal{C} = hf(u_i).$$

This is the same representation of the f term as in the finite difference method. The term \mathcal{C} contains the evaluations of the integrand at the ends weight $\frac{1}{2}$, needed to make a true Trapezoidal rule:

$$\mathcal{C} = \frac{h}{2}f(u_0)\varphi_i(0) + \frac{h}{2}f(u_{N_n})\varphi_i(L).$$

The answer $hf(u_i)$ must therefore be multiplied by $\frac{1}{2}$ if $i = 0$ or $i = N_n$. One can alternatively use the Trapezoidal rule on the reference cell and assemble the contributions. It is a bit more labor in this context, but working on the reference cell is safer as that approach is guaranteed to handle discontinuous derivatives of finite element functions correctly, while the rule was derived with the assumption that f is continuous at the integration points.

Again reconsidering equation (3.7) we can get

$$M\alpha'(t) + A\alpha(t) = \int_0^1 f \left(\sum_{j=0}^{N-1} \alpha_j(t)\phi_j(x) \right) \phi_i(x)dx - \tau\phi_i(0),$$

where $\alpha(t) = (\alpha_0(t), \alpha_1(t), \dots, \alpha_{N-1}(t))^T \in \mathbb{R}^N$ is the unknown vector. Applying one-dimensional **Gaussian Quadrature** formula in the right hand side of equation (3.7) and choosing $n = 2$ we get the approximation,

$$\begin{aligned} & \int_0^1 f \left(\sum_{j=0}^{N-1} \alpha_j(t)\phi_j(x) \right) \phi_i(x)dx \\ & \approx \frac{1}{2} \left(f \left(\sum_{j=0}^{N-1} \alpha_j(t)\phi_j\left(\frac{1}{2} + \frac{1}{2\sqrt{3}}\right) \right) \phi_i\left(\frac{1}{2} + \frac{1}{2\sqrt{3}}\right) + f \left(\sum_{j=0}^{N-1} \alpha_j(t)\phi_j\left(\frac{1}{2} - \frac{1}{2\sqrt{3}}\right) \right) \phi_i\left(\frac{1}{2} - \frac{1}{2\sqrt{3}}\right) \right) \end{aligned}$$

For Gaussian Quadrature formula we refer to the book [12].

4.2 Time Integration

In numerical analysis, we use explicit or implicit methods for getting the approximations to the solutions of time dependent ordinary and partial differential equations. Implicit method is more complex compared to the explicit method because in implicit method we need to do extra calculation. For stiff problems, we use generally implicit method because stiff equations are equations where certain implicit methods perform better, usually tremendously better, than explicit ones.

Equation (2.27) is our 1D case reaction-diffusion equation. This problem is a stiff problem. For getting the approximations to the solutions of (2.27) we apply **Implicit Euler** method. The Neumann boundary conditions are zero automatically there, since these are natural boundary conditions, that's why this term is not needed anymore.

In chapter 2, we described Brusselator model which is our 2D reaction-diffusion equation for simulation. Brusselator model is a mild stiff problem. That's why for getting the approximations to the solutions of Brusselator model we apply **Explicit Euler** method.

For stiff and general algebraic problems we refer to the book [8].

Chapter 5

Numerical Simulation

For numerical simulation, we use FEniCS project which is an open source software and a user-friendly tool for solving partial differential equations (PDEs) which is mainly written in Python/ C^{++} . It makes great use of symbolic expressions and allows to define simulations using a source code, which closely follows the mathematical formulation of the problem. For more information about FEniCS, we refer to the official FEniCS book [17].

5.1 Designs and Components of FEniCS

The FEniCS Project is structured as an umbrella project for a cluster of practical components. The main components are the followings, see [4] for more details:

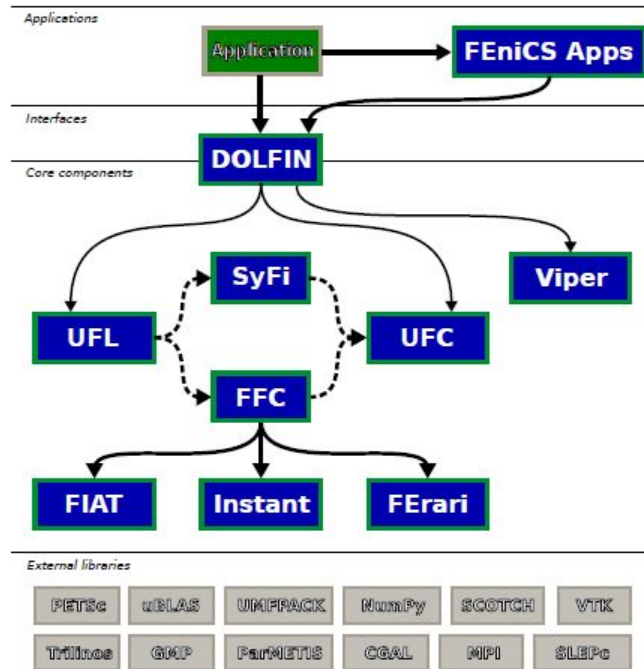


Figure 5.1: DOLFIN functions as the main user interface of FEniCS and handles the communication between the various components of FEniCS and external software. Solid lines indicate dependencies and dashed lines indicate data flow. This figure is taken from [4].

- UFL (Unified Form Language) is a domain defining language which can submerge in Python for describing finite element discretizations of differential equations in terms of finite element variational forms;
- FIAT (Finite element Automatic Tabulator) is the finite element backend of FEniCS which is a Python module;
- FFC (FEniCS Form Compiler) is a compiler for finite element variational forms which can generate UFL code as input and UFC output;
- UFC (Unified Form-assembly Code) is a C^{++} interface which is made up with low-level functions for assessing and constructing finite element variational forms;
- Instant is a Python module for aligning C and C^{++} code in Python;
- DOLFIN is a C^{++} /Python library which can provide data structures and algorithms for finite element meshes, automated finite element assembly, and numerical linear algebra.

5.2 Simulation of a Reaction-Diffusion Equation: 1D Case

We want to simulate example 2 equation (2.27) through FEniCS which we described in chapter 2. To startwith, we import dolfin, matplotlib.pyplot, numpy and math library. We create mesh and function space. After that we define sub domain for Dirichlet boundary condition, parameters, variational problem, boundary conditions. The weak form of our PDE translate to the FEniCS code using operators and inner products. The symbolic tools from FEniCS automatically translate this weak formulation into the unified form language(UFL), for which efficient assembly routines exist. For time integration we use implicit Euler because equation (2.27) is a stiff problem.

```
-----
from dolfin import *
import matplotlib.pyplot as plt
import numpy as np
import math
N = 50
# Create mesh and function space
mesh = UnitIntervalMesh(N)
V = FunctionSpace(mesh, "CG", 1)
plot(mesh)
plt.show()
# Sub domain for Dirichlet boundary condition
class DirichletBoundary(SubDomain):
    def inside(self, x, on_boundary):
        return on_boundary and near(x[0], 1.0)
# Define parameters
alpha = Constant(1.0)
delta = Constant(20.0)
R = Constant(5.0)
D = R*exp(delta)/(alpha*delta)
# Define variational problem
T = Function(V)
v = TestFunction(V)

g = Expression("0.0", degree=2)
T0 = Expression("1.0", degree=2 )
```

```

# type of T_n is of type Function(V)
T_n = project(T0, V)

# Define boundary condition
bc = DirichletBC(V, Expression( "1.0", degree=2), DirichletBoundary())

dt = 0.001

def f(T, D , alpha, delta):
    return (D * (1 + alpha - T) * exp( - delta / T))

F = 1./dt * (T - T_n)*v*dx - ( -dot(grad(T), grad(v))*dx + f(T, D, alpha, delta)*v*dx)
#T_ = Function(V)
t0 = 0.0
t_end = 0.4

T.assign(T0)
T_n.assign(T0)
t = 0.

sol_t = []
n_steps = round(t_end/dt)
sol_y = np.zeros((N+1,n_steps))
i = 0

while t < t_end:
    solve(F == 0, T, bc)
    T_n.assign(T)
    t += dt

    sol_y[:,i] = np.flip(T_n.vector().get_local())
    sol_t.append(t)

plt.plot( np.linspace(0., 1., N+1), sol_y[:,i], color=(i/n_steps,1-i/n_steps,0,1))

```

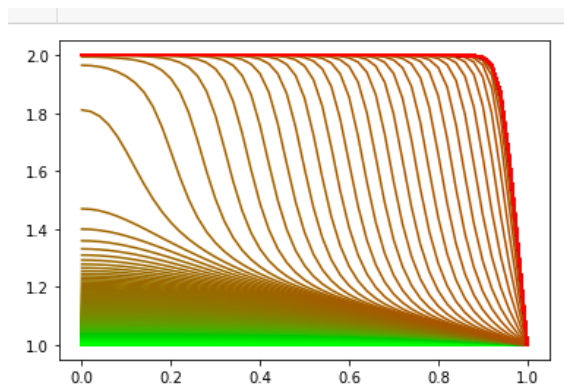


Figure 5.2: Numerical simulation result of 1D case reaction-diffusion equation.

From the above simulation result we can conclude that the temperature, initially one for all x in the domain, gradually increases with a maximum occurring at $x = 0$. Ignition occurs at a finite time, and the temperature at $x = 0$ increases rapidly to $(1 + \alpha)$. A steep front then forms and propagates toward $x = 1$ with a speed proportional to $.5e^{\alpha\delta(1+\alpha)^{-1}}$. Once the flame reaches $x = 1$, the solution reaches at a steady state. See [14].

```
-----
from matplotlib import cm
from matplotlib.ticker import LinearLocator
from mpl_toolkits.mplot3d import Axes3D
fig, ax = plt.subplots(subplot_kw={"projection": "3d"})

grid_x, grid_t = np.meshgrid(np.arange(0., 1., step=1/(N+1)), sol_t)
surf = ax.plot_surface(grid_x, grid_t, sol_y.T, cmap=cm.coolwarm,
                      linewidth=0, antialiased=False)

ax.set_zlim(0.5, 2.1)
ax.zaxis.set_major_locator(LinearLocator(10))
plt.xlabel("a")
plt.ylabel("t")
plt.show()
-----
```

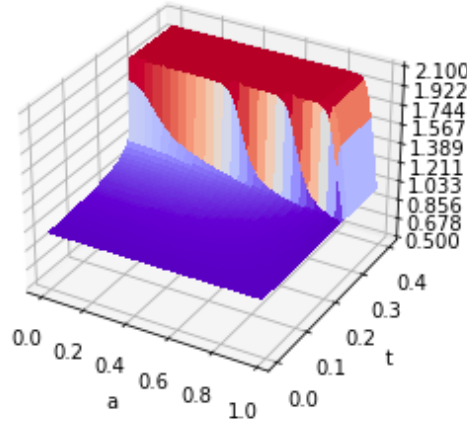


Figure 5.3: 3D visualization of 1D reaction-diffusion equation simulation result.

5.3 Simulation of a Reaction-Diffusion Equation: 2D Case

We want to simulate Brusselator model through FEniCS which we described in chapter 2. To start with, we import dolfin and matplotlib.pyplot library. We create mesh and function space. After that we define finite elements spaces and build mixed space, sub domain for Dirichlet boundary condition, parameters, variational problem, boundary conditions. The weak form of our PDE translate to the FEniCS code using operators and inner products. The symbolic tools from FEniCS automatically translate this weak formulation into the unifiedform language(UFL), for which efficient assembly routines exist. For time integration we use explicit Euler because Brusselator model is a mild stiff problem.

```

-----
from dolfin import *
import matplotlib.pyplot as plt
import numpy as np
# Create mesh and function space
mesh = UnitSquareMesh(30,30)

# Define finite elements spaces and build mixed space
CG= FiniteElement("CG", mesh.ufl_cell(), 1)
V = FunctionSpace(mesh, CG)
M = FunctionSpace(mesh, CG* CG)

plot(mesh)
# Sub domain for Dirichlet boundary condition
def DirichletBoundary(x, on_boundary):
    return False
# Define parameters
A = 3.4
B = 1
alpha = 0.002

# Define variational problem
u = Function(M)
u_1, u_2 = split(u)

v = TestFunction(M)
v_1, v_2 = split(v)
# Define boundary condition
bc = DirichletBC(M, (Constant(0.0), Constant(0.0)), DirichletBoundary)
u_10 = Expression("2 + 0.25*x[1]", degree=2)
u_20 = Expression("1 + 0.8*x[0]", degree=2)

u_1n = interpolate(u_10, V)
u_2n = interpolate(u_20, V)
dt = 0.01
F = ((u_1 - u_1n)*v_1*dx + alpha*dt*dot(grad(u_1), grad(v_1))*dx
      - dt*(B+u_1n**2*u_2n - (A+ 1)*u_1n)*v_1*dx + (u_2 - u_2n)*v_2*dx
      + alpha*dt*dot(grad(u_2), grad(v_2))*dx
      - dt*(A*u_1n - u_1n**2*u_2n)*v_2*dx)
t0 = 0.0
t_end = 5

t = 0.0

counter = -1
while t < t_end:
    solve(F == 0, u, bc)
    t += dt

    (u_1_tmp, u_2_tmp) = u.split(True)
    u_1n.assign(u_1_tmp)
    u_2n.assign(u_2_tmp)
    counter += 1
    if counter % 100 == 0:

```

```

plot(u_1n, mode = "contour")

c = plot(interpolate(u_1n, V), mode='color')
plt.colorbar(c)
plt.savefig(f'fig_{int(t)}.png')
plt.show()

```

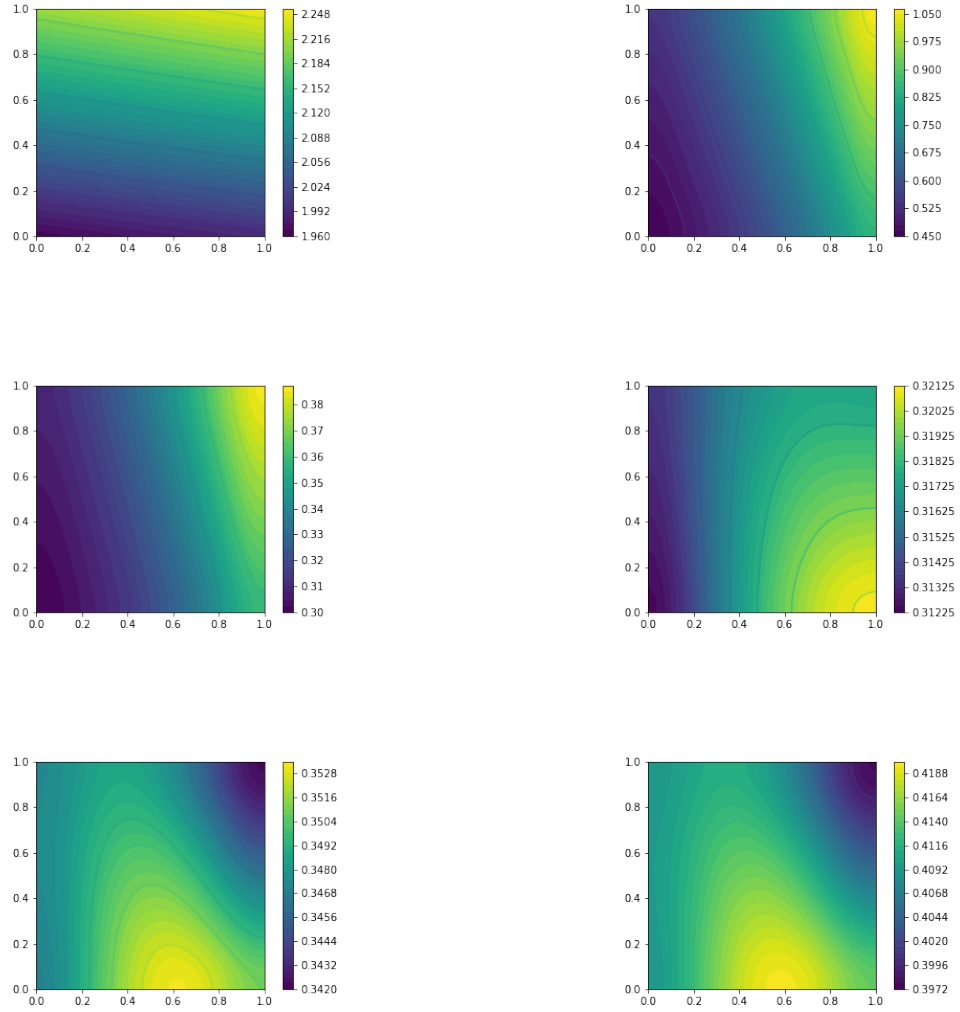


Figure 5.4: Numerical simulation result of Brusselator model at different time step.

From the simulation result of the Brusselator model, we can conclude that Brusselator model leads an oscillator to the system. After sufficient time, the oscillations approach a limit cycle which is used to model the behavior of many real-world oscillatory systems.

Chapter 6

Conclusion

In this thesis, we tried to solve reaction diffusion equations by the finite element method with FEniCS . At the beginning we derived the weak formulation and we explained the existence and the uniqueness of the reaction-diffusion equation. We choose two examples of 1D and 2D cases reaction-diffusion equations for our numerical simulation.

We explained space discretization of 1D and 2D cases reaction-diffusion equation. We also choose two applications of reaction-diffusion equation. One is the Belousov-Zhabotinskii reaction is a quite famous chemical reaction system which is able to show up oscillation and another one is Turing pattern formation which was proposed as a mechanism for pattern formation relying on the complex interaction between reaction and diffusion of some chemicals.

We discussed the treatment of non linear term by the finite element basis function, the group finite element method. We also showed how the numerical integration of non linear term can be treated by hand. For time integration we used Implicit Euler for 1D case reaction-diffusion equation and for 2D case we used Explicit Euler.

Finally, we got the simulation result of 1D and 2D cases reaction-diffusion equation. From simulation result we can conclude that at different time stepping size the solution propagates. The analysis of the numerical simulation in this work is still missing. A possible improvement on this would be to obtain the probabilistic rate of reactions of these chemical species from experimental data. This will result in a new pattern for the chemical reactions.

Bibliography

- [1] T. Porntaveetus P.T. Sharpe S. Kon M.A. Basson A. Gritli-Linde M.T. Cobourne J.A. Green A.D. Economou, A. Ohazama. *Periodic Stripe Formation by a Turing Mechanism Operating at Growth Zones in the Mammalian Palate*. Nature Genetics 44 (2012) 348-351.
- [2] Robert A. Adams. *Sobolev Spaces*. Academic Press. 1975.
- [3] G. ADOMIAN. *The Diffusion-Brusselator Equation*.
- [4] Garth N. Wells Anders Logg, Kent-Andre Mardal. *Automated Solution of Differential Equations by the Finite Element Method*. The FEniCS Book.
- [5] Dietrich Braess. *Finite Elements, Cambridge University Press, Third Edition*. 2007.
- [6] N. Britton. *Reaction-Diffusion Equations and Their Applications to Biology*. Academic Press, 1986.
- [7] Philippe G. Ciarlet. *The Finite Element Methods for Elliptic Problems*. North-Holland Publishing Company, Amsterdam, New York, Oxford, Tokyo, First Edition. 1987.
- [8] G.Wanner E.Hairer. *Solving Ordinary Differential Equations II*. Second Revised Edition.
- [9] Lawrence C. Evans. *Partial Differential Equations, SECOND EDITION AMS*. 2010.
- [10] Jacob Fish and Ted Belytschko. *A First Course in Finite Elements*. John Wiley and Sons. 2007.
- [11] P. Grindrod. *The Theory and Applications of Reaction-Diffusion Equations*. Oxford University Press, 1996.
- [12] Thomas J.R. Hughes. *The Finite Element Method*. Linear Static and Dynamic Finite Element Analysis.
- [13] Carsten Carstensen Jochen Albrety and Stefan A. Funken. *Remarks Around 50 Lines of Matlab: Short Finite Element Implementation*.
- [14] L.R. Petzold K.E.Brenan, S.L. Campbell. *Numerical Solution of Initial-Value Problems in Differential-Algebraic Equations*.
- [15] Christina Kuttler. *Reaction-Diffusion Equations with Application*. Sommersemester 2011.
- [16] Hans Petter Langtangen. *Solving Nonlinear ODE and PDE Problems*.
- [17] Hans Petter Langtangen and Anders Logg. *Solving PDEs in Python*. Springer, 2017.
- [18] L.R.Petzold. *Observations on an Adaptive Moving Grid Method for One-dimensional Systems of Partial Differential Equations*. 1987.
- [19] J. Murray. *Mathematical Biology, II: Spatial Models and Biomedical Applications*. Springer, 2003.

- [20] G. Nicolis and I. Prigogine. *Self-Organization in Nonequilibrium Systems*, Wiley-Interscience. 1977.
- [21] I. Prigogine and R. Lefever. *Symmetry Breaking Instabilities in Dissipative Systems*, *J. Chem. Phys.* 48, 1695 (1968).
- [22] S.Adjerid and J.E. Flaherty. *A moving Finite Element Method with Error Estimation and Refinement for One- dimensional Time Dependent Partial Differential Equations*. 1986.
- [23] S.I.A.M. *News* (1993).
- [24] Bernd Simeon. *Numerical Partial Differential Equations I, lecture notes at the TU Kaiserslautern*. Summer Term 2018.
- [25] Nils Hendrik Kroger Toyohiko Aiki Adrian Muntean Yosief Wondmagegne Ulrich Giese Surendra NepaL, Robert Meyer. *A moving Boundary Approach of Capturing Diffusants Penetration into Rubber: FEM Approximation and Comparison with Laboratory Measurements*.
- [26] C. Surulescu. *Reaction Diffusion Equations with Applications in Biology and Medicine*, lecture notes at the TU Kaiserslautern. Winter Term 2018/2019.
- [27] Christina Surulescu. *Mathematical Biology*. lecture notes at the TU Kaiserslautern, Summer Term 2019.
- [28] Vidar Thomee. *Galerkin Finite Element Methods for Parabolic Problems*. volume 1054. Springer, 1984.
- [29] A.M. Turing. *The chemical Basis of Morphogenesis*. Phil. Trans. R. Soc. Lond. B 237 (1952) 37-72.
- [30] J. Tyson. *Some Further Studies of Nonlinear Oscillations in Chemical Systems*, *J. Chem. Phys.* 58, 3919 (1973).
- [31] J.G.Verwer W.Hundsdoerfer. *Numerical Solution of Time-Dependent Advection-Diffusion-Reaction Equations*. Springer.